



Assessing mean climate change signals in the global CORDEX-CORE ensemble

Claas Teichmann¹ · Daniela Jacob¹ · Armelle Reca Remedio¹ · Thomas Remke¹ · Lars Bunte-meyer¹ · Peter Hoffmann¹ · Arne Kriegsmann¹ · Ludwig Lierhammer¹ · Katharina Bülow¹ · Torsten Weber¹ · Kevin Sieck¹ · Diana Rechid¹ · Gaby S. Langendijk¹ · Erika Coppola² · Filippo Giorgi² · James M. Ciarlo^{2,3} · Francesca Raffaele² · Graziano Giuliani² · Gao Xuejie^{4,5} · Taleena Rae Sines² · Jose Abraham Torres-Alavez² · Sushant Das² · Fabio Di Sante² · Emanuela Pichelli² · Russel Glazer² · Moetasim Ashfaq⁶ · Melissa Bukovsky⁷ · Eun-Soon Im⁸

Received: 8 January 2020 / Accepted: 9 October 2020
© The Author(s) 2020

Abstract

The new Coordinated Output for Regional Evaluations (CORDEX-CORE) ensemble provides high-resolution, consistent regional climate change projections for the major inhabited areas of the world. It serves as a solid scientific basis for further research related to vulnerability, impact, adaptation and climate services in addition to existing CORDEX simulations. The aim of this study is to investigate and document the climate change information provided by the CORDEX-CORE simulation ensemble, as a part of the World Climate Research Programme (WCRP) CORDEX community. An overview of the annual and monthly mean climate change information in selected regions in different CORDEX domains is presented for temperature and precipitation, providing the foundation for detailed follow-up studies and applications. Initially, two regional climate models (RCMs), REMO and RegCM were used to downscale global climate model output. The driving simulations by AR5 global climate models (AR5-GCMs) were selected to cover the spread of high, medium, and low equilibrium climate sensitivity at a global scale. The CORDEX-CORE ensemble has doubled the spatial resolution compared to the previously existing CORDEX simulations in most of the regions (25km (0.22°) versus 50km (0.44°)) leading to a potentially improved representation of, e.g., physical processes in the RCMs. The analysis focuses on changes in the IPCC physical climate reference regions. The results show a general reasonable representation of the spread of the temperature and precipitation climate change signals of the AR5-GCMs by the CORDEX-CORE simulations in the investigated regions in all CORDEX domains by mostly covering the AR5 interquartile range of climate change signals. The simulated CORDEX-CORE monthly climate change signals mostly follow the AR5-GCMs, although for specific regions they show a different change in the course of the year compared to the AR5-GCMs, especially for RCP8.5, which needs to be investigated further in region specific process studies.

Keywords Regional climate change · IPCC reference regions · CORDEX · CORDEX-CORE

Electronic supplementary material The online version of this article (<https://doi.org/10.1007/s00382-020-05494-x>) contains supplementary material, which is available to authorized users.

Claas Teichmann
claas.teichmann@hzg.de

¹ Climate Service Center Germany (GERICS), Helmholtz-Zentrum Geesthacht, Fischertwiete 1, 20095 Hamburg, Germany

² The Abdus Salam International Center for Theoretical Physics (ICTP), Strada Costiera 11, 34135 Trieste, Italy

³ National Institute of Oceanography and Experimental Geophysics (OGS), 34010 Sgonico, Italy

⁴ Climate Change Research Center, Institute of Atmospheric Physics, Chinese Academy of Sciences, Beijing, China

⁵ University of Chinese Academy of Sciences, Beijing, China

⁶ Oak Ridge National Laboratory, Oak Ridge, TN, USA

⁷ National Center for Atmospheric Research, Boulder, CO, USA

⁸ Hong Kong University of Science and Technology, Hong Kong, China

1 Introduction

Climate change is posing major challenges to society and climate change impacts are expected to increase in the near, as well as long-term future (e.g., IPCC AR5). Societal stakeholders and decision-makers need science-based climate information to adapt to expected impacts adequately and to build the resilient societies of tomorrow (Lemos 2012, Street, 2015). At the basis of reliable, science-driven climate information lie climate projections by climate models. Regional climate models (RCMs) provide high-resolution simulations on climatological timescales, typically until the year 2100. Up to this point, the multi-model ensembles of RCMs covering a large share of the regions worldwide provide climate change projections at approximately 50 km (0.44° gridbox length) spatial resolution (Jacob et al. 2014; Giorgi and Gutowski 2015; Gutowski et al. 2016). This spatial scale is insufficient for applications such as agriculture, water management or urban areas. To enable science-based decision-making and to advance the understanding of regional processes, an ensemble of high-resolution simulations across the globe is required. To meet this demand, the Coordinated Output for Regional Evaluations (CORE) (Gutowski et al. 2016) was initiated in the frame of the World Climate Research Programme (WCRP) Coordinated Regional Climate Downscaling Experiment (CORDEX) community (CORDEX-CORE). One of the aims of the CORDEX-CORE effort is to produce a coordinated set of downscaled regional climate information for the major inhabited regions of the world at unprecedented resolution and of reasonable ensemble size in order to support vulnerability, impact, adaptation and climate services applications (e.g., Ruane et al. 2016) and to enable detailed regional climate change assessments and process studies. This is especially important in those areas in which only few high-resolution simulations or only comparatively coarse simulations from global models were available so far.

As a useful outset, the regional climate model REMO and RegCM are the first participating models in the CORDEX-CORE ensemble (Jacob et al. 2012; Jacob and Podzun 1997; Giorgi et al. 2012). The initial CORDEX-CORE dataset provides projections at a spatial scale of approximately 25 km (0.22°) for RCP2.6 and RCP8.5 from 2006–2100 (including the historical time period from 1971–2005), as well as ERA-Interim driven simulations between 1979–2017 for evaluation of the performance of the models in the different CORDEX-CORE domains (Remedio et al. 2019). The data is open without restriction and can be accessed in the Earth System Grid Federation (ESGF)¹. Nine CORDEX-CORE

domains are simulated by the CORDEX-CORE RCMs; Africa (AFR-22), Central America (CAM-22), South America (SAM-22), East Asia (EAS-22), Southeast Asia (SEA-22), South Asia (WAS-22), North America (NAM-22), Australia (AUS-22), Europe (EUR-11). For the European domain there are already simulations available at approximately 12.5km (0.11°) grid resolution (Jacob et al. 2014), which are used in several studies to assess the performance of RCMs and regional climate change in Europe (e.g., Vautard et al. 2014; Prein et al. 2016; Knist et al. 2017; Kjellström et al. 2018; Teichmann et al. 2018). To present the state-of-the-art available knowledge, this paper includes the EUR-11 simulations that are driven by the CORDEX-CORE GCMs for REMO and RegCM. The driving global climate models (GCMs) selected for the CORDEX-CORE ensemble offer a broad spread of global equilibrium climate sensitivities (ECS), covering high, medium, and low ECS, and were based on the suitability for the dynamical downscaling (McSweeney et al. 2015). The GCM NorESM is characterised by a low climate sensitivity, the GCM MPI-ESM is characterised with a medium global ECS and HADGEM2ES is characterised with a comparatively high ECS. The RCMs and respective model combinations have been widely used and tested in many regions across the globe and therefore provide a solid starting point for the CORDEX-CORE ensemble. In addition, the evaluation simulations of the CORDEX-CORE domains have been analysed for REMO by Remedio et al. (2019). It is intended that the CORDEX-CORE ensemble can then be extended by additional regional simulations to further increase the ensemble size and thus the representation of possible future climate change pathways.

In the frame of this paper, we want to introduce and analyse the CORDEX-CORE ensemble of regional climate simulations. Mean climate changes in different areas of the world are investigated, based on the newly defined IPCC physical climate reference regions (Iturbide et al. 2020). The analysis focuses on the mean climate change signals of the near-surface temperature and precipitation. For selected regions, the study compares available global climate change information of the Coupled Model Intercomparison Project (CMIP5) GCM ensemble including its ensemble spread to the new CORDEX-CORE simulations, particularly focusing on the driving GCMs and their representation of the entire AR5 ensemble. This evaluation of the CORDEX-CORE dataset in comparison to other available climate information is pivotal to understand the newly added information, as well as to highlight differences among the available information to the so-called Vulnerability, Impacts, Adaptation and Climate Services (VIACS) communities and other climate information users. In addition, the CORDEX-CORE ensemble of regional climate information will allow new areas of research, which were not possible to be investigated before.

¹ e.g., at <https://esgf-data.dkrz.de/search/cordex-dkrz/>.

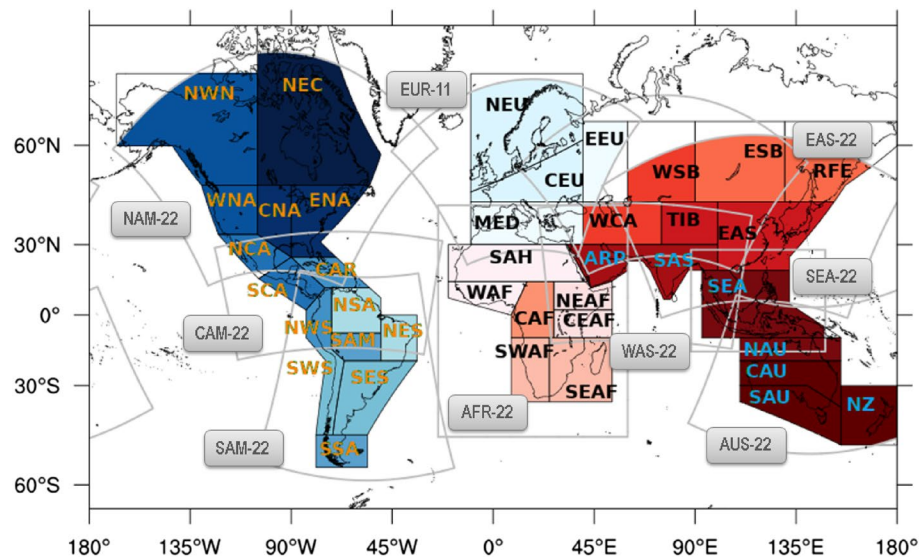


Fig. 1 The CORDEX-CORE domains (gray borders) and regions of analysis based on the AR6 IPCC physical climate reference regions (black polygons). The regions are defined as follows: N.E. Canada (NEC), C. North America (CNA), E. North America (ENA), N.W. North America (NWN), W. North America (WNA), N. Central America (NCA), S. Central America (SCA), Caribbean (CAR), N.W. South America (NWS), South America Monsoon (SAM), S. South America (SSA), S.W. South America (SWS), S.E. South America (SES), N. South America (NSA), N.E. South America (NES), N. Europe (NEU), C. Europe (CEU), E. Europe (EEU), Mediterranean (MED), W. Africa (WAF), Sahara (SAH), N.E. Africa (NEAF), C.E.

Africa (CEAF), S.W. Africa (SWAF), S.E. Africa (SEAF), C. Africa (CAF), Russian Far East (RFE), E. Siberia (ESB), W. Siberia (WSB), W.C. Asia (WCA), Tibetan Plateau (TIB), E. Asia (EAS), Arabian Peninsula (ARP), S. Asia (SAS), S.E. Asia (SEA), N. Australia (NAU), C. Australia (CAU), S. Australia (SAU), New Zealand (NZ). The CORDEX domains are: North America (NAM-22), Central America (CAM-22), South America (SAM-22), Europe (EUR-11), Africa (AFR-22), South Asia (WAS-22), East Asia (EAS-22), Southeast Asia (SEA-22), and Australasia (AUS-22) (Iturbide et al. 2020; Gutowski et al. 2016)

For example, using CORDEX-CORE, it will now be possible to assess future climate (mean, extremes and hazards) worldwide at an unprecedented resolution of 0.22° using an homogeneous, consistent ensemble, e.g., (Ciarlo et al. 2020; Coppola et al. 2020; Weber et al. 2020). It also complements the ensemble of RCM simulations for regions with a small ensemble size (e.g., Central America (Cavazos et al. 2020)). In addition, it will be possible to study one phenomena across multiple domains (e.g., monsoons, tropical cyclones) and to assess the consistency of climate change signals and possible added values (in comparison with coarser resolution simulations which are already existing) in follow-up studies. Last but not least, the high-resolution climate change information for the major inhabited regions of the world aims at enabling and feeding into regional and global climate change assessments, such as the upcoming IPCC AR6 Report.

2 Data and methods

The CORDEX-CORE ensemble run high-resolution simulations over nine CORDEX domains (Fig. 1). In this figure, 39 regions out of the 55 IPCC reference regions are covered by the CORDEX-CORE domains and used for analysing

the climate change signals in these domains. The associated domains of these regions were selected according to its areal majority. For example, the Northwest South America (NWS) region is associated with the South American domain (SAM-22), because it is best covered by the SAM-22 domain. In this regional analysis, only the land points are considered.

The RCM simulations performed in the frame of this study were done using the regional climate models REMO (RCM1) and RegCM (RCM2). The model configuration details are listed in Table 1. According to the CORDEX-CORE experimental guidelines (CORDEX Scientific Advisory Team 2019), the downscaling was conducted to a horizontal resolution of $0.22^\circ \times 0.22^\circ$ (approx. $25 \times 25 \text{ km}^2$) except for the European domain, where the EURO-CORDEX experimental guidelines were adapted at a horizontal resolution of $0.11^\circ \times 0.11^\circ$ (approx. $12.5 \times 12.5 \text{ km}^2$).

The small RCM ensemble was driven by a core set of GCMs (Table 2) from the Coupled Model Intercomparison Projects Phase 5 or CMIP5 (Taylor et al. 2012) that cover low, medium, and high equilibrium climate sensitivity (ECS). The REMO and RegCM simulations were mainly driven by the NorESM1-M, MPI-ESM-LR, and HadGEM2-ES, which are referred to as primary CORDEX-CORE GCMs in the following. However, the RegCM simulations

Table 1 The regional climate models (RCMs) configuration in the present CORDEX-CORE Ensemble

	RCM1: REMO	RCM2: RegCM
Model version	REMO2015 (Jacob et al. 2012; Remedio et al. 2019)	RegCM4 (Giorgi et al. 2012)
Institution	GERICS	ICTP
Grid resolution	$0.22^\circ \times 0.22^\circ$	$25 \text{ km} \times 25 \text{ km}$
Vertical levels	27	23
Map projection	Rotated pole lat-lon	Oblique Mercator
Planetary boundary layer	Monin-Obukhov similarity theory (Louis 1979)	Holtslag PBL (Holtslag et al. 1990)
Cumulus	Tiedtke (1989) with modifications from Nordeng (1994) and Pfeifer (2006)	Tiedtke (1989)
Microphysics	Lohmann and Roeckner (1996)	SUBEX (Pal et al. 2000)

The two participating institutions are Climate Service Center Germany (GERICS), Helmholtz-Zentrum Geesthacht, Hamburg, Germany and the Abdus Salam International Centre for Theoretical Physics (ICTP), Trieste, Italy

Table 2 The CMIP5 global climate models (GCMs) used as driving fields in the present CORDEX-CORE Ensemble

	Name	Institution	Horizontal resolution	Vertical levels	References
GCM-L1	NorESM1-M	NCC	$1.8947^\circ \times 2.5^\circ$	26	Bentsen et al. (2013)
GCM-L2	GFDL-ESM2M	GFDL	$2.0225^\circ \times 2.5^\circ$	48	Dunne et al. (2012)
GCM-M1	MPI-ESM-LR	MPI-M	$1.8653^\circ \times 1.875^\circ$	47	Giorgetta et al. (2013)
GCM-M2	MPI-ESM-MR	MPI-M	$1.8653^\circ \times 1.875^\circ$	95	Giorgetta et al. (2013)
GCM-H1	HadGEM2-ES	MOHC	$1.25^\circ \times 1.85^\circ$	38	Jones et al. (2011)
GCM-H2	MIROC5	AORI, NIES, JAMSTEC	1.4008×1.40625	49	Watanabe et al. (2010)

The horizontal and vertical resolution refers to the atmospheric component of the GCMs. The institutions affiliated to the GCMs are the following: Norwegian Climate Centre (NCC), Geophysical Fluid Dynamics Laboratory (GFDL), Max Planck Institute for Meteorology (MPI-M), Met Office Hadley Centre (MOHC), and Atmosphere and Ocean Research Institute, the University of Tokyo (AORI), National Institute for Environmental Studies (NIES), Japan Agency for Marine-Earth Science and Technology (JAMSTEC)

were alternatively driven by GFDL-ES2M, MPI-ESM-MR, and MIROC5 in selected domains, which are referred to as secondary CORDEX-CORE GCMs.

The complete list of simulations available in this study are listed in Table 3. The model version as well as domain size and RCM/GCM combinations analyzed in this study are indicated in the table. Due to time limitations, only the simulations available at the ESGF were considered. At each model domain, the number of ensemble members is between three and six.

The climate variables investigated in this study were precipitation and the near surface temperature (temperature at 2m height). The simulations were evaluated for the historical period. For the observed climatology, we used the Climatic Research Unit (CRU) temperature and precipitation version CRU TS 4.02 dataset (Harris et al. 2014). The spatial coverage included all land areas excluding Antarctica at 0.5° resolution. The period considered in this study was from 1971 to 2000.

The model biases were mainly evaluated against the CRU observational dataset. The RCM simulations were interpolated to the CRU grid (0.5° resolution) using bilinear remapping functions from the Climate Data Operators version 1.9.7 (Max

Planck Institute for Meteorology 2006). The absolute biases of the simulated monthly precipitation and near surface temperature were calculated compared to the observed monthly values. For the relative bias, the mean absolute bias was normalised with the observed climatological mean. The mean absolute and relative biases were then aggregated into the CORDEX-CORE IPCC reference regions (Fig. 1). The simulated temperature values were height-corrected to account for the differences in the orography between the RCMs and CRU.

The projected mean changes in near-surface temperature and precipitation were calculated based on the historical period from 1971 to 2000. The mean climate changes are calculated for the near-future (2036 to 2065) or far-future (2070 to 2099) minus the historical period.

3 Results

The results are divided into historical evaluation, climate change signals and GCM and RCM climate change signals in IPCC reference regions.

Table 3 The list of available RCM simulations for the CORDEX-CORE Ensemble

Domains	Model version	Size	RCM/GCM Combinations
NAM-22	REMO2015	305 × 255	RCM1-L1, RCM1-M1, RCM1-H1
	RegCM4.4	372 × 278	RCM2-L2, RCM2-M1, RCM2-H1, (all for RCP8.5 only)
CAM-22	REMO2015	417 × 225	RCM1-L1, RCM1-M1, RCM1-H1
	RegCM4.7	573 × 343	RCM2-L2, RCM2-M2, RCM2-H1
SAM-22	REMO2015	285 × 345	RCM1-L1, RCM1-M1, RCM1-H1
	RegCM4.7	330 × 360	RCM2-L1, RCM2-M2, RCM2-H1
AFR-22	REMO2015	385 × 417	RCM1-L1, RCM1-M1, RCM1-H1
	RegCM4.7	477 × 497	RCM2-L1, RCM2-M2 (RCP8.5 only for near-future), RCM2-H1
EAS-22	REMO2015	417 × 255	RCM1-L1, RCM1-M1, RCM1-H1
	RegCM4.4	381 × 247	RCM2-L1, RCM2-M2, RCM2-H1, (simulations were incomplete at the time of analysis)
SEA-22	REMO2015	273 × 201	RCM1-L1, RCM1-M1, RCM1-H1
	RegCM4.7	335 × 189	RCM2-L1, RCM2-M2, RCM2-H1
WAS-22	REMO2015	385 × 255	RCM1-L1, RCM1-M1, RCM1-H1
	RegCM4.7	429 × 337	RCM2-L1, RCM2-M2, RCM2-H2
AUS-22	REMO2015	417 × 255	RCM1-L1, RCM1-M1, RCM1-H1
	RegCM4.7	413 × 335	RCM2-L1, RCM2-M2, RCM2-H1
EUR-11	REMO2015	424 × 412	RCM1-L1, RCM1-H1
	REMO2009	424 × 412	RCM1-M1
	RegCM4.6	527 × 527	RCM2-M1 (RCP8.5 only), RCM2-H1

The simulation matrix is composed of two RCMs in combination with six GCMs: REMO/NorESM1-M (RCM1-L1), REMO/MPI-ESM-LR (RCM1-M1), REMO/HadGEM2-ES (RCM1-H1), RegCM/NorESM1-M (RCM2-L1), RegCM/GFDL-ESM2 (RCM2-L2), RegCM/MPI-ESM-LR (RCM2-M1), RegCM/MPI-ESM-MR (RCM2-M2), RegCM2/HadGEM2-ES (RCM2-H1), RegCM2/MIROC5 (RCM2-H2) over nine domains using the low (RCP2.6) and high (RCP8.5) emission scenarios. The future climate periods considered in this study are: 2036–2065 (near-future) and 2070–2099 (far-future)

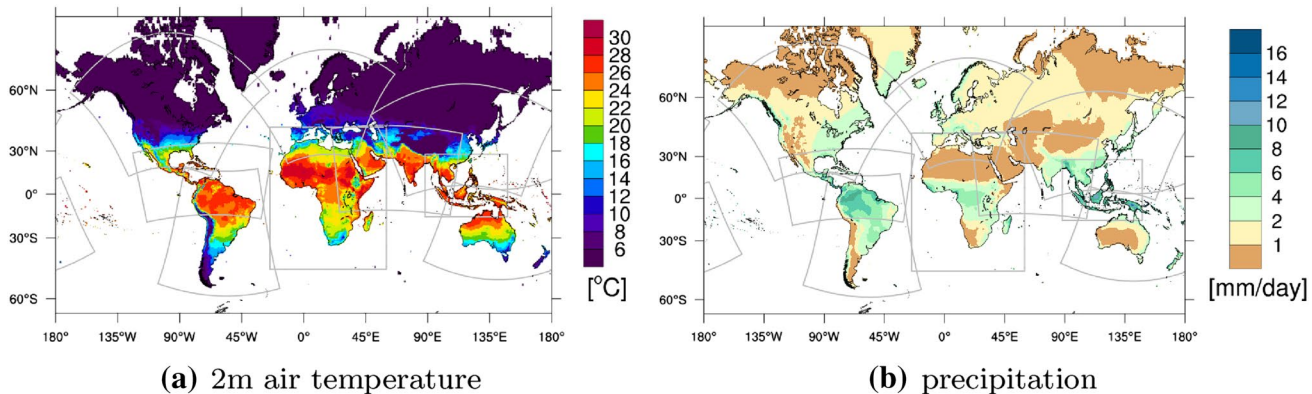


Fig. 2 Mean annual near surface temperature (a) and precipitation (b) based on the Climatic Research Unit (CRU) TS 4.02 observational dataset during the period 1971 to 2000. The domain boundaries are depicted in gray polygons

3.1 Historical evaluation

The observed mean annual near-surface temperature and precipitation are shown in Fig. 2. The climate during the historical period (1971 to 2000) is classified by warm or cold and wet or dry regions.

The RCMs are evaluated together with its corresponding GCMs during the historical period from 1971 to 2000. The RCM simulations were interpolated to the CRU observational dataset at 0.5° resolution. To compare the GCMs with CRU, the observational dataset were interpolated to the coarser GCM grid. For the near surface temperature bias

calculation, a height correction was applied to the dataset that was interpolated to account for the height difference between the observation and simulations.

The simulations are compared to the CRU observational dataset for the 39 IPCC reference regions (Fig. 1) used in this study. Fig. 3 shows the mean annual biases of temperature and precipitation of the RCMs and their driving GCMs compared to CRU (Fig. 2). The range of the biases for the GCMs is about -3.1 to 2.6 K while for the RCMs it is about -6.4 to 1.9 K (Fig. 3). For the GCMs with a low climate sensitivity, both NorESM (GCM-L1) and GFDL (GCM-L2) tend to have more regions with cold biases than warm. The magnitude of these biases were generally reduced in REMO (RCM1-L1) with exceptions of 7 regions (SES, EEU, SAH, ESB, WSB, CAU, SAU). The biases in RegCM (RCM2-L1 and RCM2-L2) are also reduced compared to the biases of the GCM-L1 and GCM-L2 with exceptions of 6 regions (CNA, ENA, WNA, NCA, SCA, and SAS), where the model have a tendency of more than 2K cold bias.

For the GCMs with the medium climate sensitivity, both MPI-ESM-LR (GCM-M1) and MPI-ESM-MR (GCM-M2) have generally more regions with cold biases compared to CRU but the number of regions with warm biases increased compared to GCM-L1 and GCM-L2. The magnitudes of the biases were reduced in more than 20 regions in REMO, with exceptions of the cold biases of both REMO (RCM1-M1) and RegCM (RCM2-M1 and RCM2-M2) in regions of the North America and Central America domain (ENA, NCA, SCA). The RegCM simulations tend to have a strong cold bias (more than -2 K) in these regions.

A comparison of 2m temperature simulated by RCM1-M1 at a coarser spatial resolution of 0.44° shows that the signs of the biases are also negative for SAH and WAF (Teichmann et al. 2013). In the evaluation of the relative precipitation biases for SWAF and SEAF, the authors also found negative values for the coarser spatial resolution in those regions. However, it should be noted that a comparison with such analyses in existing literature is difficult because they are often using different reference periods, observational data sets or sub-regions.

For the GCMs with the high climate sensitivity, most of the regions have a cold bias against CRU in HadGEM-ES (GCM-H1) while most of the regions have a warm bias against CRU in the MIROC5 (GCM-H2). The magnitude of these biases were reduced in REMO (RCM1-H1) except for some regions in the Australasia domain (CAU and SAU). In most of the regions simulated by RegCM (RCM2-H1 and RCM2-H2) the magnitude of the biases are larger than the biases of the driving GCMs (GCM-H1 and GCM-H2) especially in the already mentioned regions over the North American domain (CNA, ENA, NWN, NCA).

The precipitation biases of the simulations compared to CRU (Fig. 3b) show a large region dependency and are

less dependent on the driving GCMs. The GCM simulations have a bias range of -80 to more than 1000 % while the RCM simulations have a bias range of -67 to 638 %. In regions with a 30-year average precipitation of less than 1 mm/day (Fig. 2b), the precipitation is largely exacerbated in the GCM simulations (e.g., SAH and SWS). These biases were substantially reduced in the RCM simulations. In other dry regions like SSA, SWAF and TIB, the wet biases in the RCM simulations were either similar to the GCM simulations or reduced.

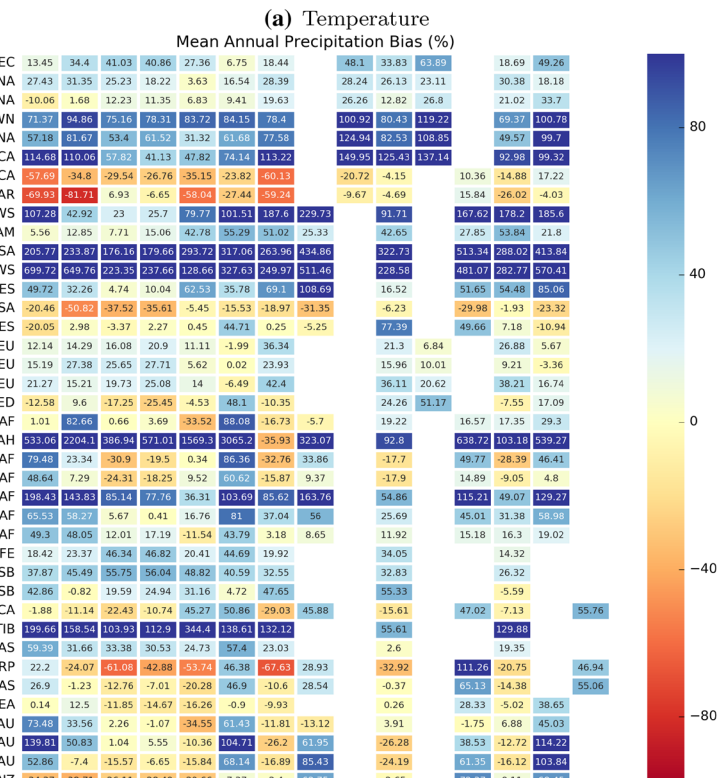
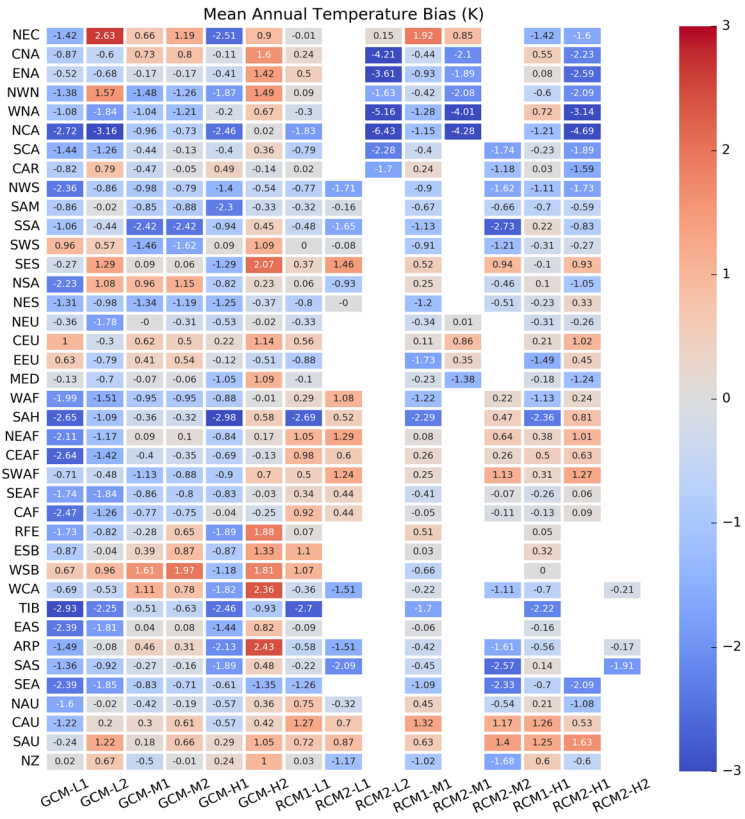
The cause for the presented biases of temperature and precipitation in the specific regions can be due to different reasons: 1) biases related to large scale processes (inherent to some extent in the GCM forcing; e.g., atmospheric circulation, SST biases, etc.) and 2) biases related to small scale processes (e.g., orographic features, convection, etc.). Even when applying techniques intended to reduce such biases (e.g., subsequent bias adjustment, bias adjusting GCM SSTs prior to downscaling) model biases will persist and, finally, the choice on the need for bias adjustment needs to be decided wisely and tailored to the application (i.e. the result will depend on the bias adjustment methodology and the observational dataset used). Therefore, we do not provide any generalized recommendations on the need for bias adjustment of the CORDEX-CORE ensemble in this context.

3.2 Global climate change signals

The near-future and far-future mean annual climate change signal for each of the RCM simulations driven by the six GCM simulations are shown in the supplementary material. In this subsection, the ensemble mean climate signals for all the available RCM simulations are shown. For each RCP, the number of ensemble members range from three to six RCM simulations.

In order to assess the significance of the climate change signals of the CORDEX-CORE ensemble in each region of the world, the two-sided Mann-Whitney-U test (Mann and Whitney 1947) is applied for each gridbox and each simulation. The reference period is compared to one respective future climate period and is counted as significant on a 95 % confidence level. The choice of the confidence level is guided by Tebaldi et al. (2011). In case that all CORDEX-CORE simulations show a significant climate change signal of the same direction, the climate change signal of the ensemble is defined as significant and robust, and appears hatched in the horizontal plots. The combined criterion for significance and robustness can be regarded as strict - in particular the robustness criterion expecting agreement in sign without exception - but is chosen because of the small CORDEX-CORE ensemble size at this moment in time.

Fig. 3 Heat maps of annual mean temperature [K] and precipitation biases [%] averaged over the area of the 39 IPCC reference regions for the period 1971 to 2000. The x-axis are the 6 driving GCMs and RCMs and the y-axis are the IPCC reference regions defined in Fig. 1. The following abbreviations are used: GCM-L1 (NorESM1-M), GCM-L2 (GFDL-ESM2M), GCM-M1 (MPI-ESM-LR), GCM-M2 (MPI-ESM-MR), GCM-H1 (HadGEM2-ES), GCM-H2 (MIROC5), RCM1 (REMO), and RCM2 (RegCM)



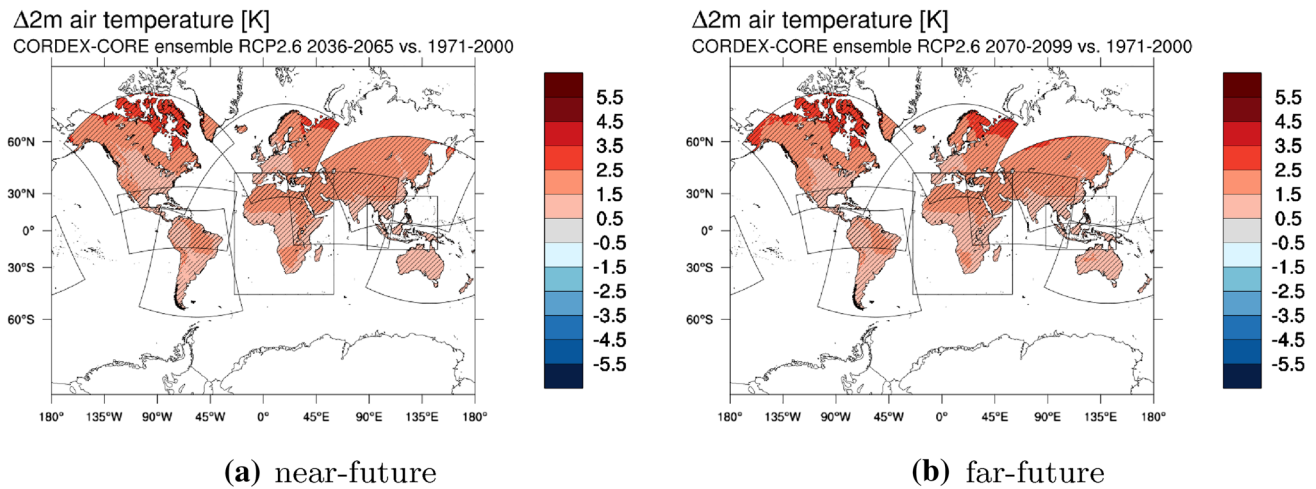


Fig. 4 The CORDEX-CORE ensemble mean near surface temperature climate change signal driven by GCMs using the RCP2.6 scenario for the near-future (2036–2065; left panel) and the far-future

(2070–2099; right panel) compared to the historical period (1971–2000). Areas that show a significant and robust climate change signal as defined in Sect. 3.2 are hatched

3.2.1 Absolute near surface temperature climate change signal

The climate change signal of the CORDEX-CORE ensemble for the low-end scenario (RCP2.6) during the mid-century (near-future) and end-century (far-future) periods are depicted in Fig. 4. For this scenario, the ensemble mean near surface temperature climate change signals vary regionally from +0.5 to +3.5K for both the near-future and far-future time periods. The areas with the highest climate change signal of more than +2.5K are the northern tips of the North American and European domains during the near-future time period (Fig. 4a) and extended to the northern tip of the East Asian domain during the far-future time period (Fig. 4b). Significance and robustness of those climate change signals is present across all domains, except for limited areas in South America and North Australia during the near-future time period. However, during the far-future time period significance and robustness manifests for these limited areas as well.

Analogous, the climate change signal of the CORDEX-CORE ensemble for the high-end scenario (RCP8.5) during the mid-century (near-future) and end-century (far-future) periods are depicted in Fig. 5. For this scenario, the ensemble mean near surface temperature climate change signals vary regionally from +0.5 to +4.5K during the middle of this century (Fig. 5a), while this signal increases globally by about 1K by the end of this century (Fig. 5b). Significance and robustness of those climate change signals is present across all domains and during both the near-future and far-future time periods.

3.2.2 Absolute and relative precipitation climate change signal

To investigate the climate change signals of the CORDEX-CORE ensemble for precipitation, both the absolute as well as the relative change signals are shown in Fig. 6 and Fig. 7 for the the low-end scenario (RCP2.6) and high-end scenario (RCP8.5), respectively. Absolute as well as relative changes are shown to identify potentially spurious relative signals that appear in response to small absolute changes (of about ± 0.1 mm/day) being present in very dry regions such as deserts. As for temperature, the change signals are illustrated for the middle (near-future) and end of this century (far-future).

For the low-end scenario, most of the domains in the northern hemisphere exhibit a wet climate change signal between +5 to +15 % especially over the north of the North American, European and East Asian domains. A wet climate change signal is also present over the Southeast South American (SES) region. The strong wet climate change signal over the Sahara desert is considered spurious due to a very small absolute climate change signal between ± 0.1 mm/day in this region. The CORDEX-CORE ensemble reproduced a drying of about -5 to -15 % in Central America, Northeast of Brazil, northern and southern parts of Africa. Over the Australasia domain, the weak dry signal spreads throughout the continent during the end of this century (Fig. 6d). Overall, significance and robustness of those climate change signals is limited across all domains during the near-future as well as far-future period. Nonetheless, parts of the North American domain and Northern Europe exhibit significant

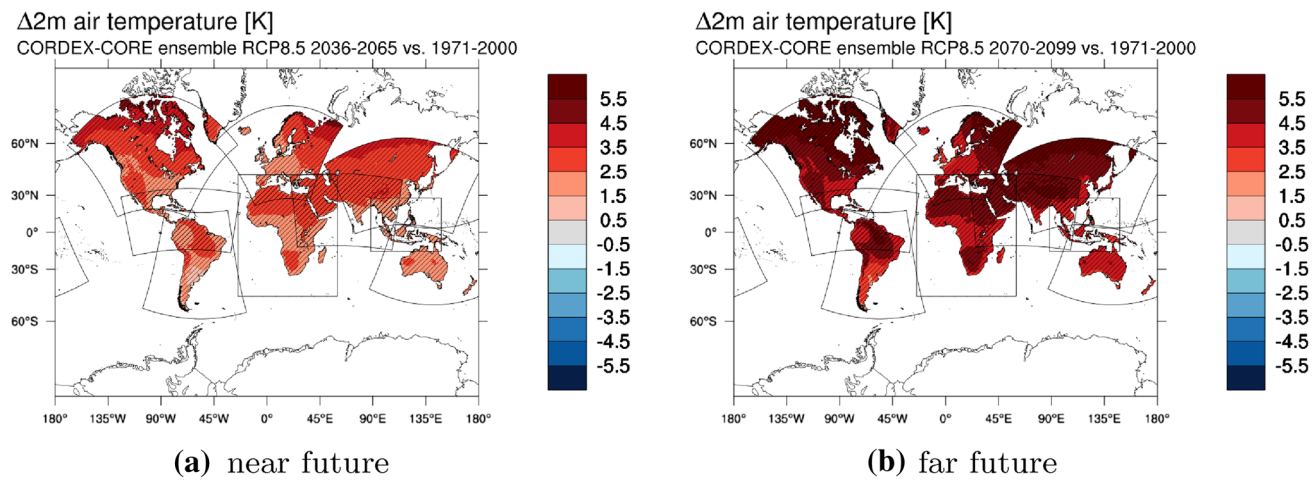


Fig. 5 The CORDEX-CORE ensemble mean near surface temperature climate change signal driven by GCMs using the RCP8.5 scenario for the near-future (2036–2065; left panel) and the far-future

(2070–2099; right panel) compared to the historical period (1971–2000). Areas that show a significant and robust climate change signal as defined in Sect. 3.2 are hatched

and robust change signals being present during both the near-future as well as far-future period.

The climate change signal of the CORDEX-CORE ensemble for the high-end scenario (RCP8.5) during the mid-century (near-future) and end-century (far-future) periods are depicted in Fig. 7. Compared to the low-emission scenario, the magnitude and coverage of the wet climate change signal across the northern hemisphere increases and expands further south. This is in particular detectable over the North American and European domains with wet signals reaching +50 % at the end of this century (Fig. 7d). In addition, similar dry signal patterns are present compared to the low-emission scenario but with increased magnitudes ranging between –15 to –50 %. One exception depicts the Australasia domain for which the dry signal expresses weaker and even a wet signal manifests over the Central Australia (CAU) region. Significant and robust change signals appear for contiguous regions over the North American and European domain (wet signal) and across parts of the Southern America domain as well as over limited areas over Southern Europe (dry signal). These regions manifest and extend during the end of this century. In addition, climate change signals over Northern and Southern Africa as well as Central America (dry signal) emerge.

To further investigate the simulated climate change signals for precipitation, the contribution of each CORDEX-CORE ensemble member is disentangled by considering individual GCM-RCM combinations. Their relative climate change signal for the high-end scenario for the end of this century is illustrated in Fig. 8. The ensemble mean wet signal observed over North America is inherent to all CORDEX-CORE ensemble members of the NAM-22 domain. Analogous, the ensemble mean dry signal over the Amazon

is inherent to all CORDEX-CORE ensemble members of the SAM-22 domain, except there is an emerging wet signal over the Northwest South America (NWS) region in the medium and high climate sensitivity driving GCMs (Fig. 8d–h). For Australia, the strong ensemble mean wet signal is dominated by the CORDEX-CORE ensemble members of the AUS-22 domain driven with NorESM1. In contrast, the ensemble mean wet signal over Southern India originates from the three REMO simulations, while the two RegCM simulations indicate a drying over this region.

3.3 GCM and RCM climate change signals in IPCC reference regions

The selection of the driving GCMs for the CORDEX-CORE RCMs was guided by the equilibrium climate sensitivity of the GCMs and thus the coverage of the spread of climate change signals of the entire AR5-GCM ensemble at global scale. As regional assessments using CORDEX-CORE ensemble data are aiming at regional to local scale, the representation of the AR5 ensemble climate change signal spread at these spatial scales is important.

In order to investigate the climate change signals at regional scales and for RCP2.6 and RCP8.5, we are focusing on the AR6 IPCC reference regions. In this paper, the ensemble spread of the entire AR5-GCMs, the driving GCMs and the CORDEX-CORE RCMs is shown for one selected IPCC reference region per CORDEX-CORE domain (see Figs. 9 and 11). The selection was guided by the representatives of the selected IPCC reference region with respect to the mean climate change signal for temperature and precipitation in the regions. In this part of the analysis we are focusing on the end of the century period (2070–2099).

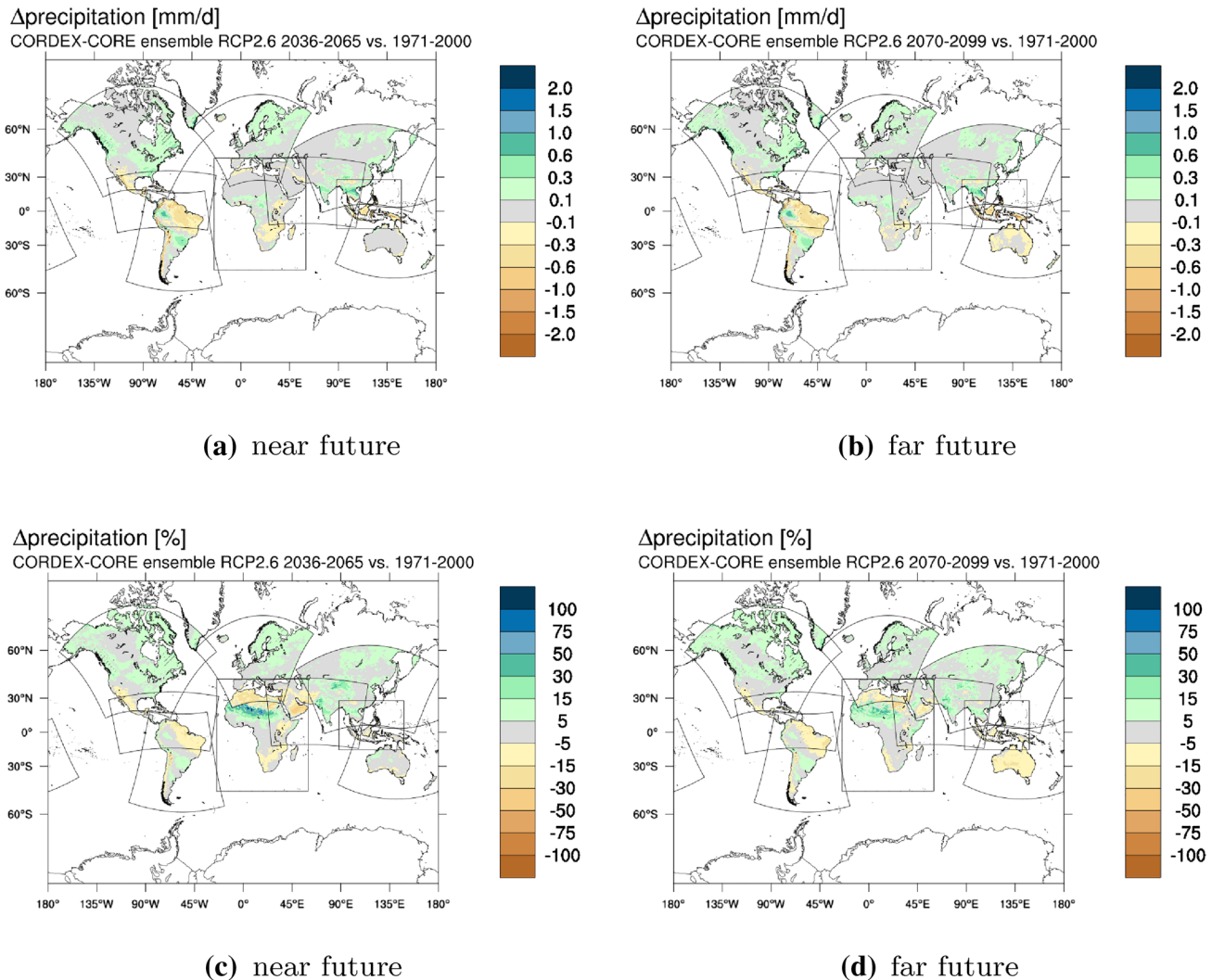


Fig. 6 The CORDEX-CORE ensemble mean precipitation climate change signal driven by GCMs using the RCP2.6 scenario for the near-future (2036–2065; left panel) and the far-future (2070–2099; right panel) compared to the historical period (1971–2000). The top

panel illustrates the absolute climate change signal in mm/day and the bottom panel the relative climate change signal in %. Areas that show a significant and robust climate change signal as defined in Sect. 3.2 are hatched

Figures for all AR6 IPCC reference regions are shown in the supplementary to this paper.

3.3.1 Temperature—annual means

The temperature climate change signals over selected IPCC reference regions are shown in Fig. 9.

For the CORDEX-CORE domain North America (NAM-22), the East North America IPCC reference region (ENA) was selected. The AR5-GCM climate change signal is covered to a large extent by the CORDEX-CORE driving GCMs as well as by the CORE RCMs for RCP2.6 and RCP8.5. The interquartile range (ranging from about +1.1K to about 2.3K for RCP2.6 and from about 4K to about 5.7K for RCP8.5) is well represented by CORE driving GCMs and CORE RCMs.

This is also the case for all other IPCC reference regions in the NAM-22 domain (see supplementary). CORE GCM climate change signals are reduced by the RCMs by up to 0.5K for RCP2.6 and by up to 1.5K for RCP8.5 in the ENA region.

For the IPCC reference region central Europe (CEU) in the EUR-11 CORDEX-CORE domain, the AR5-GCM ensemble interquartile ranges are covered by the CORE GCMs. The CORE RCMs show a slightly reduced climate change signal for all driving CORE GCMs, not reaching the upper 75th percentile of about 6K in the case of RCP8.5. In other IPCC reference regions, the interquartile ranges is well covered by CORE GCMs and RCMs, except for the Mediterranean (MED) region, where the 25th percentile is about 0.5K lower than the low ECS CORE GCM and RCM (see supplementary).

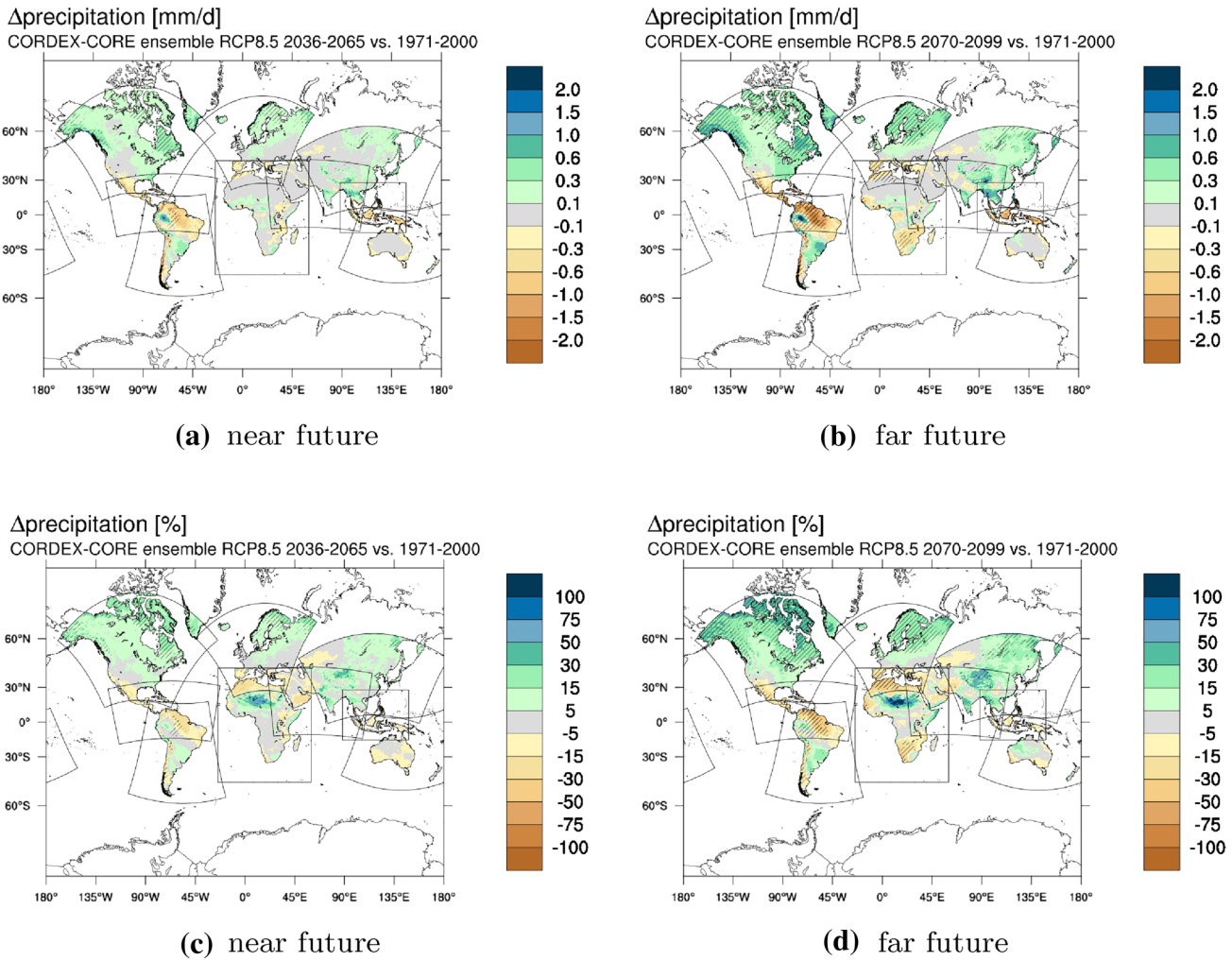


Fig. 7 The CORDEX-CORE ensemble mean precipitation climate change signal driven by GCMs using the RCP8.5 scenario for the near-future (2036–2065; left panel) and the far-future (2070–2099; right panel) compared to the historical period (1971–2000). The top

panel illustrates the absolute climate change signal in mm/day and the bottom panel the relative climate change signal in %. Areas that show a significant and robust climate change signal as defined in Sect. 3.2 are hatched

The interquartile range of the AR5-GCM ensemble climate change signal is well represented in the IPCC reference region East Asia (EAS) within the CORDEX-CORE domain EAS-22 for RCP2.6, although the lowest climate change signal is shown by the medium ECS CORE GCM and its RCM. In the case of RCP8.5, the low ECS CORE GCM shows about the same climate change signal as the AR5-GCM ensemble median of about 4.2K. The CORE RCM reduces the climate change signal by about 0.5K, in this case.

The IPCC reference region South Central America (SCA) is one of the two IPCC reference region lying within the CORDEX-CORE domain SAM-22. The AR5-GCM ensemble interquartile ranges are well covered by the CORE GCMs and the CORE RCMs. In this domain, in addition to the primary GCMs, also the secondary low and medium ESC GCMs were used for downscaling the climate change

signal in this domain. CORE RCMs show similar climate change signals (with in a range of less than 0.5K) than their driving GCMs and also the differences of the climate change signals of primary and secondary GCMs and the respective RCM climate change signals are lying within this range.

The IPCC reference region South Asia (SAS) which is covering the Indian subcontinent, lies within the CORDEX-CORE domain WAS-22. Similar to the case of the IPCC reference region SCA, which was discussed before, The AR5-GCM interquartile range is covered by CORE GCMs and CORE RCMs. Also, primary and secondary GCMs are used to drive the CORE RCMs and again, the climate change signals are similar for the CORE GCM and the CORE RCM climate change signal, i.e. they are lying within a range of 0.5K. The only exception is the high ECS GCM, showing a climate change signal of about 3.4K,

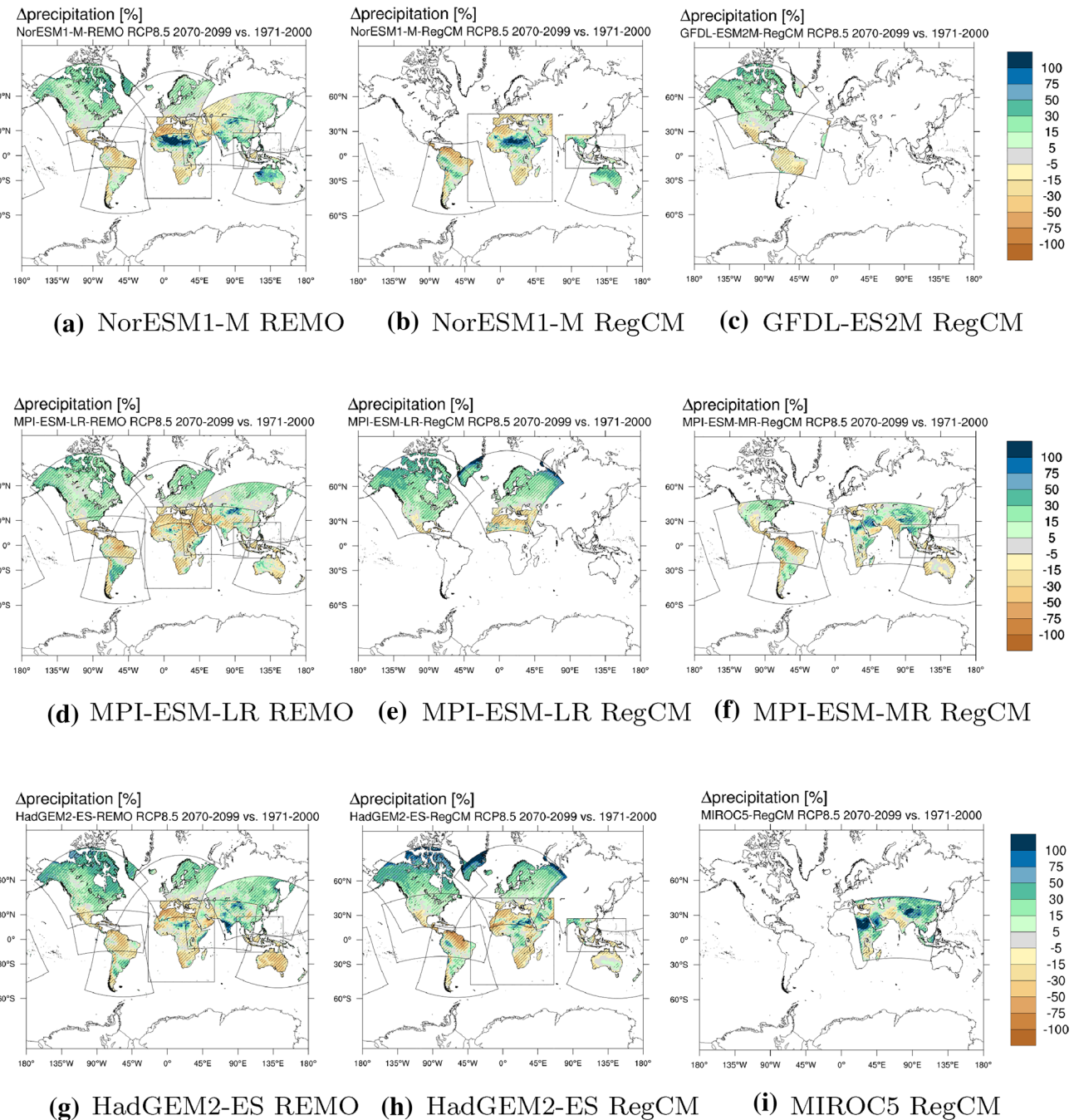


Fig. 8 Mean relative precipitation climate change signal (%) for the high emission scenario (RCP8.5) for the far-future (2070–2099) with respect to the historical reference climate (1971–2000) as simulated

by the individual RCMs driven by the six CORE GCMs. Areas that show a significant climate change signal as defined in Sect. 3.2 are

while its RCM shows a climate change signal of about 4.8K. With the exception of the latter case, also the order of low, medium and high ECS GCMs and CORE RCMs is preserved in the climate change signal.

The IPCC reference region South East Asia lies within the CORDEX-CORE domain SEA-22. The AR5-GCM

interquartile range is well covered by CORE GCMs and RCMs. The climate change signals between driving CORE GCMs and RCMs are within a range of about 0.2K and thus very similar. Also the medium ECS CORE GCMs and RCMs show a similar climate change signal. Again,

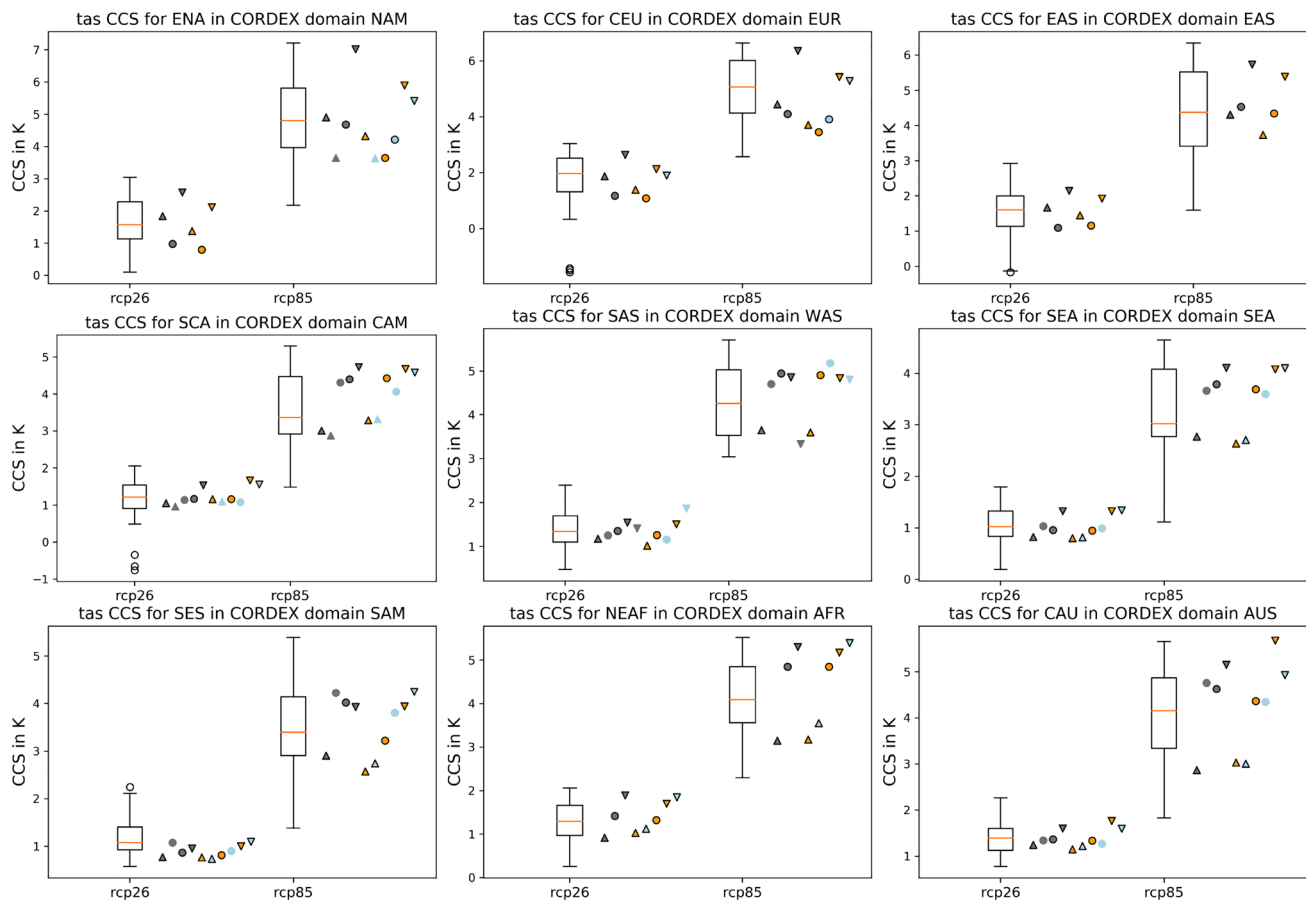


Fig. 9 Temperature climate change signals for AR5-GCMs and CORDEX-CORE RCMs in selected IPCC reference regions. Temperature climate change signals over selected IPCC reference regions are plotted for RCP2.6 and RCP8.5 at the end of the century (2020–2099) for the entire AR5-GCM ensemble, the CORDEX-CORE driving GCMs of the respective CORDEX-CORE domain and the CORDEX-CORE RCMs. The climate change signal of the AR5-GCM ensemble is depicted as a box-whisker plot. The driving AR5-GCMs with low,

the order of low, medium and high ECS CORE GCM and RCM climate change signals is preserved.

The IPCC reference region South East South America lies within the CORDEX-CORE domain SAM-22. The interquartile range in this region is very narrow of about 0.5K. CORE GCMs and RCMs show a similarly narrow spread of climate change signals for RCP2.6, but shifted towards lower climate change signals ranging between about 0.8K and 1.2K, while the median of the AR5-GCM ensemble lies at about the latter value. For RCP8.5, the interquartile range of the AR5-GCMs ensemble is well covered by CORE GCMs and RCMs. Except for the primary GCM climate change signal of about 4K and the corresponding RCM climate change signal of about 3.2K, the RCM climate change signals are within a range of about 0.2K of its driving GCMs.

medium and high equilibrium climate sensitivity are plotted as gray triangles pointing upwards, circle and triangle pointing downwards, respectively. Primary GCMs are marked with a solid border. The RCMs driven by low, medium and high equilibrium climate sensitivity GCMs are drawn using the same symbols as before, but in orange for REMO and in blue for RegCM. Primary driving GCMs are again marked with a solid symbol border

For the CORDEX-CORE domain AFR-22 the IPCC reference region North-East-Africa (NEAF) was selected. The CORE GCMs and RCMs cover the interquartile range of the AR5-GCMs. The high ECS GCMs and the corresponding CORE RCMs are close to the maximum of the AR5-GCM ensemble climate change signal of about 2.1K for RCP2.6 and about 5.5K for RCP8.5. The downscaled climate change signals are within a range of less than 0.5K compared to the driving CORE GCMs.

For the IPCC reference region Central Australia, lying in the CORDEX-CORE domain AUS-22, the interquartile range of the AR5-GCM ensemble is well covered by CORE GCMs and CORE RCMs. For both RCPs, the order of low, medium and high global ECS is reflected in the climate change signal of the CORE GCMs and RCMs, as the downscaled climate change signal lies within a range of about

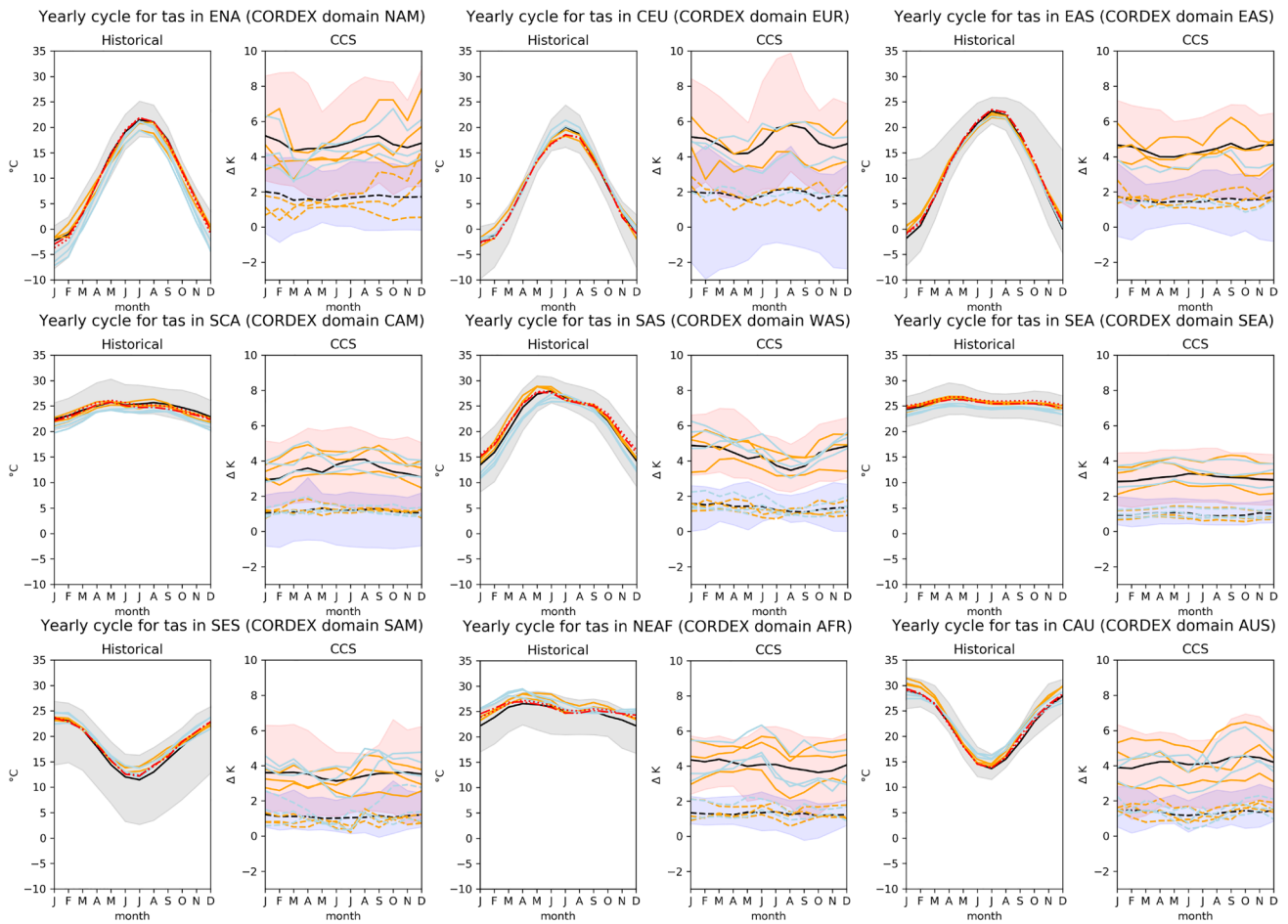


Fig. 10 Annual cycles of temperature for the historical time period and of climate change signals for AR5-GCMs and CORDEX-CORE RCMs in selected IPCC reference regions. The historical time period (1971–2000) is shown on the left hand side of each plot. Here, the gray shaded areas indicate the ranges of the entire AR5-GCM ensemble, with the black solid lines representing the ensemble median. The CORDEX-CORE RCMs REMO and RegCM are depicted as orange lines and blue lines, respectively. As a reference, the annual cycles of CRU TS4.02 (dotted red line) and ERA5 (dash-dotted red line) are illustrated. The annual cycle temperature climate change signals

0.2K for each GCM-RCM combination. Only the climate change signal of the CORE RCMs driven by the high ECS GCM differs by about 0.8K. While REMO increases the GCM climate change signal of about 5.2K to about 5.9K, RegCM decreases it slightly to about 4.9K. A similar behaviour is shown for the other IPCC reference regions in the AUS-22 domain.

In general, it is not necessarily the case that the order of global low, medium and high equilibrium climate sensitivity is preserved for each of the IPCC reference regions. In the case of the tropical IPCC reference regions the order of low, medium and high climate sensitivity is generally preserved. In addition, tropical regions show very similar

are shown for RCP2.6 and RCP8.5 for the end of this century (2070–2099) at the right hand side of each plot. Here, the shaded areas represent the climate change signals of the AR5-GCMs for RCP2.6 (blue shaded areas) and RCP8.5 (red shaded areas), with the black solid lines representing the ensemble median for RCP2.6 (dashed black lines) and RCP8.5 (solid black lines). The CORDEX-CORE RCMs REMO and RegCM are depicted as orange lines and blue lines, respectively, separated into RCP2.6 (dashed lines) and RCP8.5 (solid lines)

climate change signals in when comparing CORE RCMs with their driving CORE GCMs.

3.3.2 Temperature—annual cycles

The annual cycle temperature climate change signals (CCS) over selected IPCC reference regions are shown in Fig. 10. As a reference for the historical annual cycles simulated by the AR5-GCMs and the CORDEX-CORE RCMs we indicate the annual cycles of the ERA5 global reanalysis (Hersbach et al. 2020) and the CRU TS 4.02 dataset (Harris et al. 2014).

For the historical time period (1971–2000), the median of the AR5-GCMs is generally close to the annual cycles of the reference datasets CRU and ERA5. Only in a few regions and during specific months deviations of more than about one Kelvin are present (e.g., about -2K in region NEAF for November to February or about +2K in CEU for July). The annual temperature cycles of the RCMs are mostly within the full ranges of the GCMs and follow similar cycles throughout the year. However, in some of the regions the annual cycles of the RCMs are rather below the GCM median (ENA, EAS, SCA, SEA) while in other regions they tend to be above the AR5-GCM median (SES, NEAF, CAU).

The median of the AR5-GCM climate change signals (CCS) for the end of this century (2070–2099) are rather stable throughout the year for most of the regions, staying within a range of about +1-2K for RCP2.6 and +3-5K for RCP8.5. Only in a few regions the median climate change signal varies markedly throughout the year. This is, e.g., the case for CEU, where the median climate change signal is about +4K in April and May, while it is about +6K in July, August and September in RCP8.5. The CCS of the RCMs for RCP2.6 and RCP8.5 for the end of this century (2070–2099) are largely within the respective ranges of the CCS of the AR5-GCMs. The range of the RCM CCS is relatively narrow and centered around the GCM ensemble median. For RCP2.6, the range is usually within ± 1 K but can reach to around ± 2 K (e.g., ENA, SES) for single simulations during several months. For RCP8.5 the RCMs show larger differences. Here, the projected CCS are usually centered around the AR5-GCM ensemble median within ± 2 K. Nevertheless, there can be a difference between the RCM simulations of up to around 4K for specific regions and single months (e.g., ENA in December). Looking closer at particular regions, the ENA region indicates a wider range between the RCM CCS during fall and winter (September to February), as well as an upward trend of the CCS in those months compared to the rest of the year for both RCP2.6 and RCP8.5. The SES region is characterised by a stronger CCS from August to January, being projected by almost all RCM simulations. This is not shown by the AR5-GCM ensemble median. In the NEAF region all RCMs show a decrease in the CCS of about 1.5K between June and August for RCP8.5, which is not visible in the ensemble median CCS of the GCMs. In other regions like SCA and SEA, the CCS of the RCMs do not vary strongly throughout the year and range within ± 2 K.

3.3.3 Precipitation—annual means

The precipitation climate change signals over the selected IPCC reference regions discussed in Sect. 3.3.1 are shown in Fig. 11.

The precipitation climate change signal in the IPCC reference region ENA lies around 5% for the interquartile range

of the AR5-GCMs for RCP2.6 and around 9% for the interquartile range for RCP8.5. The interquartile range is covered by the CORDEX-CORE GCMs and their respective RCMs. RCMs only show a slight difference in climate change signal with respect to their driving GCMs of less than about 3%, except for the high ECS GCM and REMO, where the RCM shows more than about 6% more increase than the driving GCM.

For the IPCC reference region CEU, the CORE GCM and RCM climate changes signals tend to be lower than the 75th percentile for RCP2.6. CORDEX-CORE GCMs are lower than the AR5-GCM ensemble climate change signal median which is at about 4% precipitation increase, while the CORDEX-CORE RCMs show a climate change signal, which is above this value, thus showing a higher climate change signal in this region.

The precipitation climate change signals in the EAS IPCC reference region show a good coverage of the interquartile range of the AR5-GCM ensemble. The CORE GCM climate change signals are reduced by the RCMs by values between around 3% and 8%, leading to a projected decrease of precipitation by the CORE RCMs instead of an increase in precipitation as projected by the medium ECS GCM.

The median precipitation change of the AR5-GCM ensemble lies around 0% for the IPCC reference region SCA. The selected CORDEX-CORE GCMs show a precipitation climate change signal above this median value, while the corresponding CORDEX-CORE RCM climate change signals show a larger spread reaching from a decrease in precipitation of about 15% to an increase in precipitation of about 10% for RCP2.6. The projections for RCP8.5 show a good coverage of the interquartile range of the AR5-GCM ensemble by the CORDEX-CORE GCM climate change signals, which is reproduced by the CORDEX-CORE RCMs, although some climate change signals of the RCMs differ by up to 20% to their driving CORDEX-CORE GCMs (e.g., for the medium ECS GCM and REMO).

Climate change signals of the CORDEX-CORE GCMs for the SAS IPCC reference region reach from about -5% to about 13% for RCP2.6, thus covering the AR5-GCM ensemble very well. This is reflected by the CORDEX-CORE RCMs, which tend to reproduce the climate change signals of their driving GCMs by within a range of about 4%. In the case of RCP8.5 for the same region, the larger spread of AR5-GCM ensemble climate change signals is also reflected by the CORDEX-CORE GCMs but to a lesser extend, i.e. not reaching the whiskers of the boxplot representing the distribution. CORDEX-CORE RCMs reproduce the GCM climate change signal, but the extremes are more amplified, e.g., the high ECS GCM, showing an increase in precipitation of about 10% corresponds to an increase in precipitation of the downscaled RCM of about 33%.

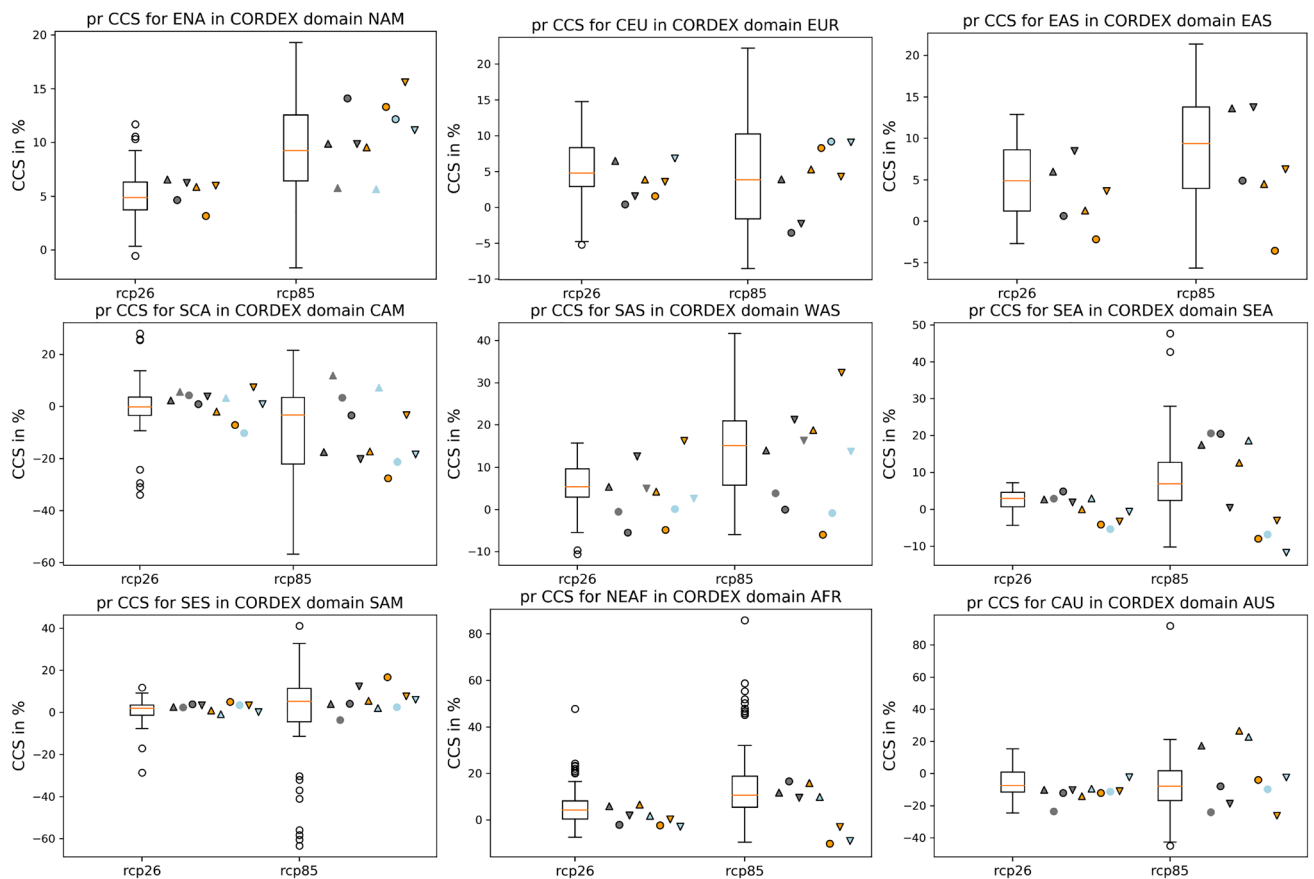


Fig. 11 Precipitation climate change signals for AR5-GCMs and CORDEX-CORE RCMs in selected IPCC reference regions. The symbols are the same as in Fig. 9

In the SEA IPCC reference region, the relatively small AR5-GCM interquartile range from about 1% to about 5% is covered by the CORDEX-CORE GCMs in RCP2.6, while the CORE RCMs generally show lower precipitation changes down to decrease in precipitation for medium and high ECS GCM driving simulations. For RCP8.5 the driving GCMs are lying outside of the interquartile AR5 ensemble range. CORDEX-CORE GCMs with low and medium ECS are lying above the 75th percentile, while the high ECS GCM lies below the 25th percentile. While RCMs driven by the low ECS GCM are lying at or above the 75th percentile, RCMs driven by the medium and high ECS GCMs are lying below the 25th percentile. Thus the spread is reflected, but the AR5-GCM ensemble interquartile range is not represented neither by the CORDEX-CORE GCMs nor by the CORDEX-CORE RCMs for RCP8.5.

For the IPCC reference region SES the AR5-GCM ensemble interquartile range is rather small ranging from about -3% to about 3% for RCP2.6 and between about -5% and about 10% for RCP8.5. CORDEX-CORE GCMs and CORDEX-CORE RCMs are lying in around this range for RCP2.6. For RCP8.5, CORDEX-CORE GCMs are

covering the interquartile range, while CORDEX-CORE RCMs show about the same climate change signals within a range of about 5%, except for the primary medium ECS GCM and the corresponding RCM, where the RCM projects more than about 15% additional increase to the increase of the GCM.

For the IPCC reference region NEAF, the AR5-GCM ensemble interquartile ranges are represented by the CORDEX-CORE GCMs for RCP2.6 and RCP8.5, except for the 25th percentile of RCP8.5, which is not represented by a CORDEX-CORE GCM. The RCMs downscaling medium and high ECS GCMs are projecting a decrease in precipitation instead of an increase as their driving GCMs.

While some of the AR5-GCMs project an increase in precipitation for RCP2.6, all CORDEX-CORE GCMs as well as all CORE RCMs (except for RegCM driven by the high ECS GCM) project a decrease in precipitation which lies below the median of about 8%. For RCP8.5, the AR5-GCM ensemble interquartile range, extending from about -18% to about 2% is well covered by the CORDEX-CORE GCMs and CORDEX-CORE RCMs. CORDEX-CORE RCMs show a higher percentage value of the climate change signal as their

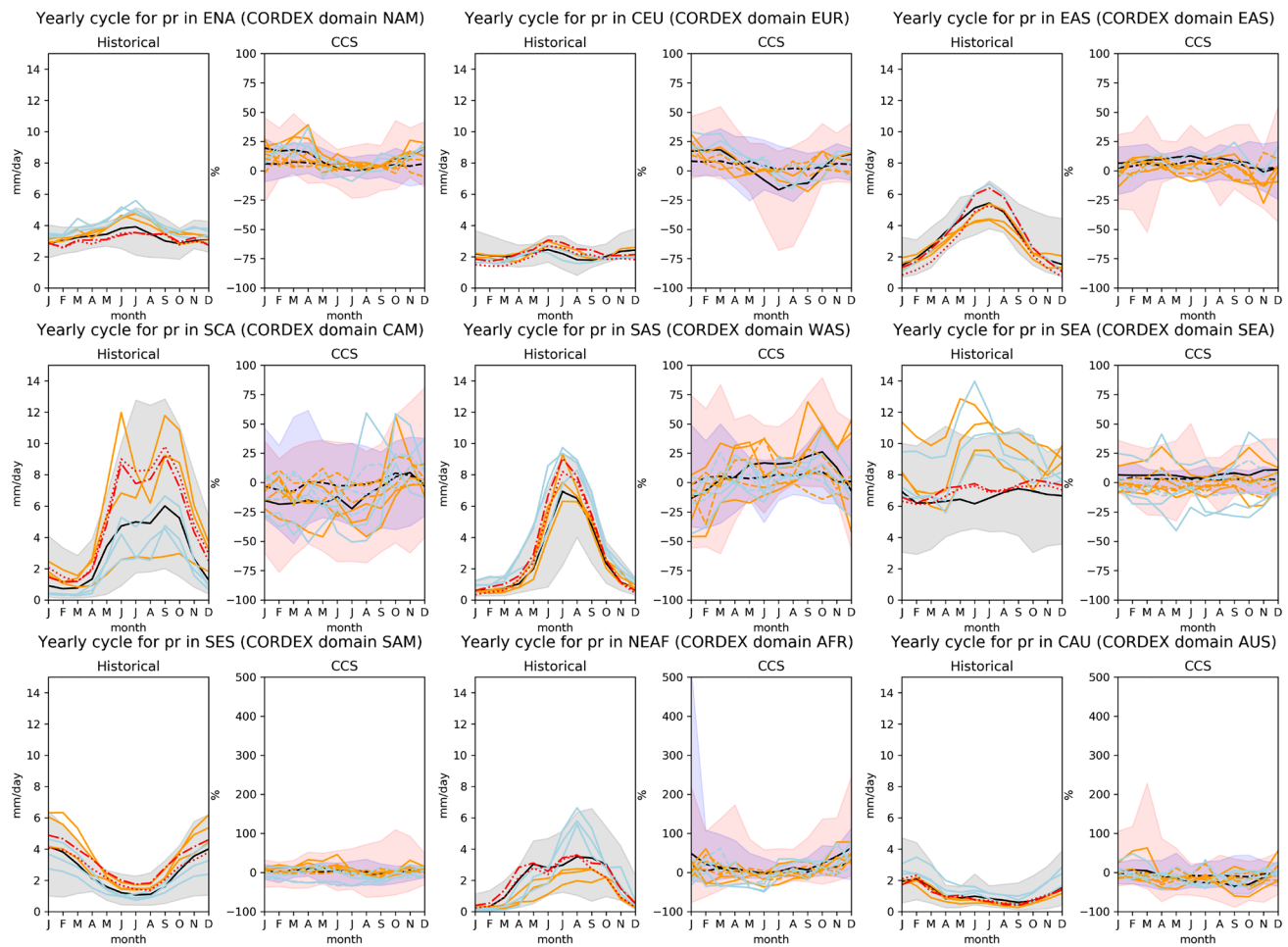


Fig. 12 Annual cycles of precipitation for the historical time period and of climate change signals for AR5-GCMs and CORDEX-CORE RCMs in selected IPCC reference regions. The historical time period (1971–2000) is shown on the left hand side of each plot. Here, the gray shaded areas indicate the ranges of the entire AR5-GCM ensemble, with the black solid lines representing the ensemble median. The CORDEX-CORE RCMs REMO and RegCM are depicted as orange lines and blue lines, respectively. As a reference, the annual cycles of CRU TS4.02 (dotted red line) and ERA5 (dash-dotted red line) are illustrated. The annual cycle precipitation climate change signals are shown for RCP2.6 and RCP8.5 for the end of this century (2070–

driving GCMs, except for the high ECS GCM downscaled by REMO, where the climate change precipitation signal is decreased from about 18% to about 34%.

3.3.4 Precipitation—annual cycles

The annual cycle precipitation climate change signals over selected IPCC reference regions are shown in Fig. 12. As for the annual cycles of temperature, the ERA5 global reanalysis (Hersbach et al. 2020) and the CRU TS 4.02 dataset (Harris et al. 2014) serve as reference for the historical annual cycles simulated by the AR5-GCMs and the CORDEX-CORE RCMs.

2099) at the right hand side of each plot. Here, the shaded areas represent the climate change signals of the AR5-GCMs for RCP2.6 (blue shaded areas) and RCP8.5 (red shaded areas), with the black solid lines representing the ensemble median for RCP2.6 (dashed black lines) and RCP8.5 (solid black lines). The CORDEX-CORE RCMs REMO and RegCM are depicted as orange lines and blue lines, respectively, separated into RCP2.6 (dashed lines) and RCP8.5 (solid lines). Please note that for the CCS the scale of the y-axis is different for the regions SES, NEAF and CAU. Monthly precipitation amounts of less than 0.01 mm/day were not considered for the AR5-GCMs

The precipitation ensemble median of the AR5-GCMs for the historical time period (1971–2000) is in general close (less than 2mm/day) to the annual cycles of the reference of CRU and ERA5. Nevertheless, in some regions, the deviations are larger. In the region SCA, e.g., differences between the AR5-GCM ensemble median and the reference are larger than 2mm/day for the months June to September and reach up to about 4mm/day. However, also a larger (more than 0.5mm/day) difference between the two reference datasets is present in this regions.

For the historical time period the shapes of the curves of the annual precipitation cycles of the RCMs are rather

similar to the annual cycles of the GCM ensemble medians throughout the year. The annual cycle as simulated by the RCMs lies within the range of AR5-GCMs for most of the RCM simulations and for most of the months of the year. In the regions SCA, SAS and SEA, a few RCM simulations show a historical monthly precipitation, which is more than 1mm/day larger than the maximum of the AR5-GCM ensemble. Such RCM simulations are outside of the GCM ranges. On the other hand there is no such deviation for the minimum precipitation amounts.

While in some regions the precipitation simulated by the RCMs tends to lie above the AR5-GCM median (e.g., ENA, SEA, SAS), in another region, it tends to lie mainly below (EAS). In the majority of the regions, the RCM simulations cover the range of the AR5-GCMs and lie above and below the AR5-GCM median. The differences between the RCM simulations can range up to 10mm/day.

The precipitation median of the AR5-GCM climate change signals at the end of the century (2070-2099) stays rather constant (within a range of about +10% and -10% points around a fixed value) and is thus rather independent of the time of the year for some regions (EAS, SEA, SES) for both RCPs. In other regions, this is only the case for RCP2.6 (NAM, CEU, SCA, SAS and AUS). In the region NEAF, the median CCS is more than +10% points larger in the months April to September than, e.g., in June, July, August.

The precipitation climate change signals (CCS) at the end of the century (2070-2099) of the RCMs for RCP2.6 and RCP8.5 are within the respective ranges of the AR5-GCM CCS. Exceptions can be found in the regions of SCA and SEA where single RCM simulations show a CCS of more than +5% points higher than the maximum CCS for a single months of the AR5-GCM ensemble, whereas in NEAF, the CCS of single RCM simulations is up to about 20% points lower than the minimum AR5-GCM CCS for June. In general, the range of the RCM CCS projections for RCP2.6 is smaller than the range of the CCS for RCP8.5 and more closely centered around the AR5-GCM CCS ensemble median. For RCP8.5 the RCMs show differences between the single simulated RCM CCS of up to about 108% points in SCA, whereas the maximum difference for RCP2.6 between RCM CCS can be found in CAU with about 70% points. Minimum differences are about 8% points in ENA for RCP8.5 and about 0.3% for RCP2.6 in the same region. In all regions the sign of the projected CCS by the RCMs can be opposite at least for some months within the annual cycle for both RCPs, while in some regions this is even the case for all the months (e.g., SAS and SEA for RCP2.6 and SEA and SES for RCP8.5).

Closely considering particular regions, for CEU the CCS annual cycle for RCP8.5 shows a decrease in precipitation in summer months (June, July and August) and an increase in precipitation in winter months (December,

January, February). This CCS annual cycle is different than for RCP2.6, though following the GCM projections, where a similar behaviour can be seen. A similar pattern can be observed for the ENA region, though with a larger spread between the CCS of the models. In the NEAF region, GCMs project a wider range of CCS than RCM CCS for both RCP2.6 and RCP8.5 in the months December to February. The RCM CCS in the NEAF region are mainly located around the GCM CCS median for RCP2.6 and show negative CCS in the months June and July. For the RCP8.5, the GCM CCS median shows an increase in precipitation of up to 50% in the months December and January. The majority RCM CCS are below the GCM CCS median and following its upward trend in the second half of the year. A comparatively strong increase in precipitation (of partly more than about 50%) is simulated by some of the RCM simulations in the second half of the year in the regions of SCA, SAS and to some extent also in SEA and NEAF.

4 Discussion

The new high resolution climate change simulations of the CORDEX-CORE ensemble are evaluated using the CRU observational dataset during the historical period (1971 to 2000). The near-surface temperature and precipitation model biases (Fig. 3) are calculated for individual regional climate model simulations (RCMs) as well as for their driving global climate model simulations (GCMs) using the IPCC physical climate reference regions (Fig. 1). The magnitude of the temperature biases from the GCMs are generally reduced by about 0.5K to 2K by the RCM simulations, especially for the regions SAM, SWS, NES, CEAF, SEAF, CAF, and EAS. South Australia (SAU) is the only region where all RCM simulations show an increase in the magnitude of the warm bias, which is inherent in the driving GCM simulations as well.

The precipitation biases of the simulations largely depend on the region analysed. In dry regions, biases of the driving GCMs are large. However, these biases are generally reduced by the RCM simulations for the regions SCA, SAH, CEAF, ESB, TIB and EAS. For West North America (WNA), North Central America (NCA) and North West South America (NWS), the RCM simulations show an increase of the magnitude of the wet bias originating from the driving GCM simulations.

It would be important to further assess the regional and temporal details of the GCM and RCM temperature and precipitation biases, ideally with high resolution observations. This could enhance our understanding of the governing processes and the scales they are representing, in reality as well as in the global and regional simulations.

Further research is needed to understand which processes are responsible for the more realistic calculation of the near-surface temperature in RCMs (see above: decrease in biases by about 0.5K to 2K) or the increased biases in South Australia. A regional study over Australia was performed with a comparably larger RCM ensemble, providing a more detailed assessment of the performance of CORDEX-CORE simulations and CORDEX-CORE climate change signals in this region (Evans et al. 2020). There could be several reasons for these changes in biases, some of them are more realistic resolved orography, land-cover and soil moisture, besides different representations of physical processes. If the temperature biases depend strongly on the spatial details of the lower boundary conditions, they should also be smaller in high-resolution GCMs, which would be interesting to assess in future studies.

The assessment of the differences of the precipitation biases seems to be more challenging due to the divergent patterns. Further detailed regional assessments and studies would be needed to gain a more complete understanding of the precipitation biases.

A comparison of the CORDEX-CORE simulations with previous studies from the various domains is limited, e.g., due to diverging definitions of the model regions, use of various reference periods and reference datasets, analyses of different spatial and temporal scales, and due to applying different forcing GCMs. Evans et al. (2020) showed that REMO CORDEX-CORE simulations have a comparably good performance with respect to precipitation over Australia and that REMO and RegCM perform well with respect to maximum temperature while showing larger biases in minimum temperature. However, they also noted that the biases depend both on the RCM and the driving GCM. Hence, the benefit of the higher resolution (i.e. 0.22° instead of 0.44° for many domains) cannot be directly derived from this analysis. Fixed boundary conditions (e.g., from the same GCM or from ERA-Interim) would be needed for such an assessment. For instance, Prein et al. (2016) and Lucas-Picher et al. (2017) used the ERA-Interim driven evaluation simulations at different resolutions to show the improvements achieved by increasing the model resolution. Nevertheless, similar features in the model biases from CORDEX-CORE and previous CORDEX simulations can be found for some of the regions. For instance, similarities to the coarser CORDEX simulations can be found over the NCA and SCA regions. Here, cold biases are simulated by the 0.44° CORDEX-CAM ensemble (Cavazos et al. 2020) and the CORDEX-CORE ensemble. The dry biases in the annual precipitation over the NSA region and in the austral summer (DJF) precipitation over the SES region simulated by the CORDEX-CORE RCMs are also present in previous 0.44° CORDEX-SAM simulations (Solman and Blázquez 2019). In contrast, over the NES region, where the CORDEX-SAM models show a

slight wet bias, the CORDEX-CORE ensemble has a larger spread in the precipitation biases, showing both wet and dry biases. Over the ENA region NA-CORDEX simulation with various resolutions (0.44°, 0.22°, and 0.11°) show a wet bias mainly in the winter season (Lucas-Picher et al. 2017), which can be also observed in the CORDEX-CORE ensemble.

The analysis of the IPCC reference regions showed that the AR5-GCM ensemble spread of the CCS is well represented by the selected driving CORDEX-CORE GCMs for most of the regions. The interquartile range of the AR5-GCM ensemble of annual mean CCS for temperature and precipitation is covered by the CORE GCM and RCM CCS for almost all IPCC reference regions reasonably well (Figs. 9 and 11). Exceptions are present, e.g., in the CEU region where the precipitation CCS of the selected CORE GCMs are located only between the 25th percentile and the median of the AR5-GCM ensemble for RCP8.5. In the annual cycle plots for CEU (refer to Fig. 12), it is visible that the CORDEX-CORE RCMs do not follow the AR5-GCMs in simulating the strong decrease in the CCS between June and September, which might be one of the reasons for the incomplete representation of the full range of the AR5-GCM CCS in this case. In this specific case, the EURO-CORDEX ensemble at 0.11° resolution offers already a large ensemble of simulations in addition to the CORDEX-CORE simulations to get a good representation of the AR5-GCM ensemble. For other regions, such as EAS, where all CORDEX-CORE GCMs lie above the AR5-GCM ensemble median for temperature CCS, it is important to perform additional simulations driven by GCMs different to the CORDEX-CORE GCMs to better cover the lower range of AR5-GCM CCS and in order to achieve a better representation of the range of possible CCS. Nevertheless, the annual cycles for temperature CCS in EAS show that the CCS as simulated by the RCMs are located around the median values of the GCM CCS throughout the year, confirming the results of the boxplots and thus not changing the shape of the annual cycle, except for the slight increase in the CCS between July and September for the RCMs and the GCM median, which indicates a tendency to a prolonged summer season. The simulation of the historical period and their relation to the reference datasets gives an indication of the performance of the simulations in the respective regions (refer to the left panel in Figs. 10 and 12). For the temperature annual cycles, the representation of the historical annual cycle is comparatively good for the AR5-GCM ensemble median and the CORDEX-CORE RCMs. In some regions, the CORDEX-CORE RCMs show the tendency towards warmer annual cycles (e.g., in the NEAF region RCM temperatures are above the AR5-GCM ensemble median), in other regions there is a tendency towards colder annual cycles (e.g., in the SCA and ENA regions most RCM simulations show

temperatures below the AR5-GCM ensemble median). Despite these differences in the historical annual cycles between RCMs and AR5-GCMs, the range in the annual cycles of the CCS is not markedly reduced. The same is true for the rather wet (ENA and SEA region) or dry (e.g., EAS region) historical annual cycles of precipitation, which also do not show a reduced range in their respective annual cycles of CCS. Nevertheless additional simulations covering the respective other part in the historical period (warmer and colder or wetter and dryer), could lead to additional CCS outside of the simulated range which is shown here.

While the CCS for temperature stays rather constant throughout the year for RCP2.6 for all regions, the CCS shows a certain seasonality for RCP8.5 for some regions, indicating projected changes in the respective annual cycles. This is, e.g., the case for the SAS region for RCP8.5, where the CCS is elevated from October to April compared to the rest of the year for the AR5-GCM median as well as for most of the CORDEX-CORE RCMs. This indicates a tendency towards a weakening of the annual cycles as the cold period is projected to get warmer while the warm period is projected to get warmer to a lesser extent. This change in CCS is similarly projected by the AR5-GCMs as well as by the CORDEX-CORE RCMs. In the CAU region, e.g., some of the CORDEX-CORE RCMs show an increase in the CCS between about July and October, which is only partly visible in the GCMs. This might lead to increased southern hemisphere spring temperatures in CAU and thus to a broadening of the annual cycles. Nevertheless, whether this specific CCS signal is robust, needs to be confirmed by additional RCM simulations and the analysis of the underlying physical processes that might be better represented by higher resolved simulations.

A similar differential CCS can also be seen in the annual cycles of precipitation for RCP8.5 in some regions (refer to Fig. 12). In the region SCA, e.g., a CCS of decreasing precipitation is simulated for RCP8.5 in about the first half of the year, while increasing precipitation is simulated in the second half of the year for the AR5-GCMs and most of the CORDEX-CORE RCMs. In this case the precipitation in the dry season between December and April would be reduced, while precipitation would be partly increase at the end of the wet season, which in addition is projected to be prolonged by some of the simulations.

In the above described cases, using only the CORDEX-CORE simulations might lead to an underestimation of the respective climate change signals or of projected changes in the seasonality. This needs to be taken into account when using the CORDEX-CORE ensemble for further analysis or VIACS applications. Additional assumptions will have to be made in order to reflect the larger range of CCS in the AR5-GCM ensemble. The analysis might also guide regional modellers to create their modelling strategy, specifically in

the selection of additional GCMs for downscaling climate projections in the respective regions.

The CCS of the driving CORDEX-CORE GCMs seem to be reproduced by the CORDEX-CORE RCMs in many areas, especially in tropical and subtropical regions. This indicates that the processes leading to the spatial and temporal mean CCS in these regions are captured by the GCMs. The RCMs do not seem to alter them by using higher spatial and temporal resolutions, as well as different parameterizations for physical processes adapted to the higher resolution. The larger temperature bias of the CORDEX-CORE GCMs compared to the CORDEX-CORE RCMs discussed above, seem to play a minor role and cancel out in the calculation of the CCS at this temporal and spatial scale. In contrast, over a specific IPCC reference region larger differences between CORDEX-CORE GCM and RCM CCS indicate that some processes are not captured by the GCMs and that the higher temporal and spatial resolution or a different description of the physical processes seem to be important. This is, e.g., the case for the EAS region. Here, the climate change signal shows an increase in precipitation for the medium ECS GCM and a decrease for the RCM REMO simulation. The RCM simulations for low and high ECS GCMs change the signal in the same direction, but show a much lower precipitation increase than their driving GCMs in this region. The sign of the signal is not changed. Regional processes at smaller scales seem to play a major role in determining the CCS even when aggregated over a comparatively large region and a period of 30 years. To further investigate the causes of these discrepancies between GCM and RCM climate change signals, an analysis of the signal changes on higher spatial and temporal scales, e.g., process based studies of phenomena like monsoon, response to ENSO, storm track changes, is needed for the individual regions. In addition, the importance of the resolution of climate models to simulate spatial and temporal mean regional climate change in specific regions could be further elucidated when comparing high-resolution GCMs with RCMs, including analysing the influence of the better resolved large scale forcing. This was to some extent done in a study over Europe and could possibly be extended over some of the regions investigated in this study (Demory et al. 2020). Also, in the case of the low radiative forcing of the RCP2.6 scenario, the RCMs follow the CCS of the driving CORDEX-CORE GCMs quite closely.

Similar to the evaluation of the biases for the current climate, it is not straight forward to compare the CORDEX-CORE results to studies from other CORDEX simulations as the setup of the simulation and the analysis are different. Nevertheless, we want to give a few examples for a comparison of the CCS in specific regions in order to get an impression of differences and similarities. For India, which is located in the WAS region, Kulkarni et al. (2020) showed

that the CORDEX-SA projected an increase in annual precipitation, with both increases in the summer monsoon season (June to September) and winter monsoon season (December to January). Based on the CORDEX-CORE ensemble, increases as well as decreases are projected for the far future, highlighting the large uncertainty for precipitation changes in this region. Additionally, a robust shift in the timing of monsoon is noted, which is attributed to pre-monsoon drying (Ashfaq et al. 2020). Similarly, Dash et al. (2015) linked the decreases in a previous RegCM experiment to weaker monsoon circulations. The increase in precipitation in the ENA region in winter simulated by the CORDEX-CORE ensemble is consistent with the results of the NA-CORDEX simulations (Karmalkar 2018). The CORDEX-CORE projections show precipitation increases over Indochina similar to the projections by the 0.22° CORDEX-SEA ensemble (Tangang et al. 2020). The increasing trend of precipitation for the Maritime Continent is only present in the REMO projections while RegCM shows both increases and decreases.

5 Conclusions

In this paper, we show that the CORDEX-CORE ensemble reproduces the AR5-GCM ensembles temporal and spatial mean climate change signals for temperature and precipitation for most IPCC reference regions across the world. Nevertheless, in a few IPCC reference regions, the AR5-GCM ensemble of climate change signals is not represented to the full extent by the CORDEX-CORE GCMs and RCMs. In these IPCC reference regions, it is advisable to perform additional simulations to extend the CORDEX-CORE ensemble to improve the coverage of possible AR5-GCM climate change signals. We also found that the lack in coverage of the AR5-GCMs historical annual cycles by the CORDEX-CORE RCMs, does not seem to lead to a reduced range in the RCM CCS. While the CORDEX-CORE RCMs simulate a rather flat annual cycle of CCS for RCP2.6 for temperature and precipitation, for RCP8.5 a varying CCS is simulated by the AR5-GCMs and CORDEX-CORE RCMs in the course of the year in some of the investigated regions. This could potentially lead to a respective qualitative change in the annual cycle, e.g., prolonging wet or dry periods. In some regions, the annual cycle of the RCMs reflect what is projected by the AR5-GCMs, but in other regions the CCS of AR5-GCMs and RCMs are qualitatively different.

To assess the causes of regional differences in AR5-GCM and CORDEX-CORE RCM projected CCS and to investigate in detail the physical processes is out of the scope of this paper, which is rather to give an overview over the performance and the projected changes in the different regions of the world. For many applications and analyses,

CORDEX-CORE offers a reasonable ensemble of climate simulations, particularly in regions where up to now only a limited number of regional climate model simulations were available. In contrast to the GCM simulations, the CORDEX-CORE ensemble provides simulations on higher spatial and temporal resolutions, allowing for regional to local climate and impact assessments, as well as VIACS applications in the major inhabited regions of the world, while being at the same time consistent with the large scale AR5-GCM CCS. This is supported by Ciarlo` et al. (2020), who compared simulated precipitation from the EURO-CORDEX and CORDEX-CORE ensembles to the precipitation from the respective driving GCMs and found an added value mainly in complex topographical areas, coastal areas, islands and tropical regions, especially for extremes. Nevertheless, in order to fill the presented knowledge gaps and to get a better understanding of the origins of regional features, we encourage further regional process studies using CORDEX, CORDEX-CORE and ideally additional even higher resolved regional climate simulations. Ideally these additional simulations are guided by VIACS applications. This study focuses on temperature and precipitation variables. The coverage of the ensemble spread of the AR5-GCM ensemble might be different for other variables or indices and should be assessed before using the CORDEX-CORE ensemble. This is to some extent done in other papers of this special issue (e.g., Coppola et al. 2020).

We conclude that the CORDEX-CORE ensemble is a solid starting point to provide the major inhabited areas of the world with a reasonable core ensemble of climate simulations.

We want to encourage the regional scientific communities and experts to make use of the CORDEX-CORE ensemble with their modelling experiences, observations and expertise to identify and analyse in detail regional features together with historical climate and climate change signals. Regional studies which are focusing on one domain and make use of the CORDEX-CORE ensemble, can set their results in relation to other domains via the findings presented in this study and assess their transferability. These assessments will then be of great additional benefit for regional VIACS communities as well as for regional modellers to further develop and improve regional climate models and to thus better represent climate change in regions all over the world in future simulations.

The CORDEX-CORE ensemble shall be extended in the future by additional regional simulations, in order to further increase the ensemble size and thus the regional representation of possible future climate change pathways.

Acknowledgements We would like to thank the modeling groups for computing and providing the RCM simulations in the frame of the Coordinated Regional Downscaling Experiment (CORDEX)

Framework and COmmon Regional Experiment (CORE). The CORDEX-CORE REMO simulations were performed under the GERICS/HZG share at the German Climate Computing Centre in Hamburg (DKRZ). We acknowledge DKRZ in Hamburg for providing the high-computing capacity, and the Earth System Grid Federation (ESGF) for hosting the CORDEX-CORE projections. We also acknowledge the World Climate Research Program Working Group on Coupled Modelling and all the modeling groups for computing and providing the CMIP5 which was used as boundary forcing for the CORDEX-CORE simulations. Finally, we would like to thank the reviewers for their valuable comments and suggestions.

Funding Open Access funding enabled and organized by Projekt DEAL.

Open Access This article is licensed under a Creative Commons Attribution 4.0 International License, which permits use, sharing, adaptation, distribution and reproduction in any medium or format, as long as you give appropriate credit to the original author(s) and the source, provide a link to the Creative Commons licence, and indicate if changes were made. The images or other third party material in this article are included in the article's Creative Commons licence, unless indicated otherwise in a credit line to the material. If material is not included in the article's Creative Commons licence and your intended use is not permitted by statutory regulation or exceeds the permitted use, you will need to obtain permission directly from the copyright holder. To view a copy of this licence, visit <http://creativecommons.org/licenses/by/4.0/>.

References

Ashfaq M, Cavazos T, Reboita MS, Torres-Alavez JA, Im ES, Olusegun CF, Alves L, Key K, Adeniyi MO, Tall M, Sylla MB, Mehmood S, Zafar Q, Das S, Diallo I, Coppola E, Giorgi F (2020) Robust late twenty-first century shift in the regional monsoons in regcm-cordex simulations. *Clim Dyn*. <https://doi.org/10.1007/s00382-020-05306-2>

Bentsen M, Bethke I, Debernard JB, Iversen T, Kirkevåg A, Seland Ø, Drange H, Roelandt C, Seierstad IA, Hoose C, Kristjánsdóttir JE (2013) The norwegian earth system model, noresm1-m - part 1: description and basic evaluation of the physical climate. *Geosci Model Dev* 6(3):687–720. <https://doi.org/10.5194/gmd-6-687-2013>

Cavazos T, Luna-Niño R, Cerezo-Mota R, Fuentes-Franco R, Méndez M, Pineda Martínez LF, Valenzuela E (2020) Climatic trends and regional climate models intercomparison over the cordex-cam (central america, caribbean, and mexico) domain. *Int J Climatol* 40(3):1396–1420. <https://doi.org/10.1002/joc.6276>

Ciarlo JM, Coppola E, Fantini A, Giorgi F, Gao X, Tong Y, Glazer RH, Torres Alavez JA, Sines T, Pichelli E, Raffaele F, Das S, Bukovsky M, Ashfaq M, Im ES, Nguyen-Xuan T, Teichmann C, Remedio A, Remke T, Bülow K, Weber T, Bunttemeyer L, Sieck K, Rechid D, Jacob D (2020) A new spatially distributed added value index for regional climate models: the euro-cordex and the cordex-core highest resolution ensembles. *Clim Dyn*. <https://doi.org/10.1007/s00382-020-05400-5>

Coppola E, Raffaele F, Giorgi F, Giuliani G, Xuejie G, Ciarlo J, Sines TR, Torres A, Das S, di Sante F, Pichelli E, Glazer R, Ashfaq M, Bukovsky M, Im ES, Jacob D, Teichmann C, Remedio A, Remke T, Kriegsmann A, Buelow K, Weber T, Bunttemeyer L, Sieck K, Rechid D (2020) Climate hazard indices projections based on cordex-core, cmip5 and cmip6 ensemble. *Clim Dyn* (submitted to this issue)

CORDEX Scientific Advisory Team (2019) The WCRP CORDEX Coordinated Output for Regional Evaluations (CORE) Experiment Guidelines. Available online: <http://www.cordex.org/experiment-guidelines/cordex-core/> accessed on 1 March 2019

Dash SK, Mishra SK, Pattnayak KC, Mamgain A, Mariotti L, Coppola E, Giorgi F, Giuliani G (2015) Projected seasonal mean summer monsoon over india and adjoining regions for the twenty-first century. *Theor Appl Climatol* 122(3):581–593. <https://doi.org/10.1007/s00704-014-1310-0>

Demory ME, Berthou S, Sørland SL, Roberts MJ, Beyerle U, Seddon J, Haarsma R, Schär C, Christensen OB, Fealy R, Fernandez J, Nikulin G, Peano D, Putrasahan D, Roberts CD, Steger C, Teichmann C, Vautard R (2020) Can high-resolution gcm's reach the level of information provided by 12–50 km cordex rcms in terms of daily precipitation distribution? *Geosci Model Dev Discuss* 2020:1–33. <https://doi.org/10.5194/gmd-2019-370>

Dunne JP, John JG, Adcroft AJ, Griffies SM, Hallberg RW, Shevliakova E, Stouffer RJ, Cooke W, Dunne KA, Harrison MJ, Krasting JP, Malyshev SL, Milly PCD, Phillipps PJ, Sentman LT, Samuels BL, Spelman MJ, Winton M, Wittenberg AT, Zadeh N (2012) Gfdl's esm2 global coupled climate-carbon earth system models. part i: physical formulation and baseline simulation characteristics. *J Clim* 25(19):6646–6665. <https://doi.org/10.1175/JCLI-D-11-00560.1>

Evans JP, Di Virgilio G, Hirsch AL, Hoffmann P, Remedio AR, Ji F, Rockel B, Coppola E (2020) The cordex-australasia ensemble: evaluation and future projections. *Clim Dyn*. <https://doi.org/10.1007/s00382-020-05459-0>

Giorgetta MA, Jungclaus J, Reick CH, Legutke S, Bader J, Böttiger M, Brovkin V, Crucifix T, Esch M, Fieg K, Glushak K, Gayler V, Haak H, Hollweg HD, Ilyina T, Kinne S, Kornblueh L, Matei D, Mauritsen T, Mikolajewicz U, Mueller W, Notz D, Pithan F, Raddatz T, Rast S, Redler R, Roeckner E, Schmidt H, Schnur R, Segschneider J, Six KD, Stockhausen M, Timmreck C, Wegner J, Widmann H, Wieners KH, Claussen M, Marotzke J, Stevens B (2013) Climate and carbon cycle changes from 1850 to 2100 in mpi-esm simulations for the coupled model intercomparison project phase 5. *J Adv Model Earth Syst* 5(3):572–597. <https://doi.org/10.1002/jame.20038>

Giorgi F, Gutowski WJ Jr (2015) Regional Dynamical Downscaling and the CORDEX Initiative. *Annu Rev Environ Resour* 40(1):150724171620.008. <https://doi.org/10.1146/annurev-environ-102014-021217>

Giorgi F, Coppola E, Solmon F, Mariotti L, Sylla MB, Bi X, Elguindi N, Diro GT, Nair V, Giuliani G, Turuncoglu UU, Cozzini S, Güttinger I, O'Brien TA, Tawfik AB, Shalaby A, Zakey AS, Steiner AL, Stordal F, Sloan LC, Brankovic C (2012) Regcm4: model description and preliminary tests over multiple cordex domains. *Clim Res* 52:7–29. <https://doi.org/10.3354/cr01018> <http://www.int-res.com/abstracts/cr/v52/p7-29/>

Gutowski JW, Giorgi F, Timbal B, Frigon A, Jacob D, Kang HS, Raghavan K, Lee B, Lennard C, Nikulin G, O'Rourke E, Rixen M, Solman S, Stephenson T, Tangang F (2016) WCRP COordinated Regional Downscaling Experiment (CORDEX): a diagnostic MIP for CMIP6. *Geosci Model Dev* 9(11):4087–4095. <https://doi.org/10.5194/gmd-9-4087-2016>

Harris I, Jones PD, Osborn TJ, Lister DH (2014) Updated high-resolution grids of monthly climatic observations—the CRU TS3.10 Dataset. *Int J Climatol* 34(3):623–642. <https://doi.org/10.1002/joc.3711>

Hersbach H, Bell B, Berrisford P, Hirahara S, Horányi A, Muñoz-Sabater J, Nicolas J, Peubey C, Radu R, Schepers D, Simmons A, Soci C, Abdalla S, Abellán X, Balsamo G, Bechtold P, Biavati G, Bidlot J, Bonavita M, De Chiara G, Dahlgren P, Dee D, Diamantakis M, Dragani R, Flemming J, Forbes R, Fuentes M, Geer A, Haimberger L, Healy S, Hogan RJ, Hólm E, Janisková M, Keeley

S, Laloyaux P, Lopez P, Lupu C, Radnoti G, de Rosnay P, Rozum I, Vamborg F, Villaume S, Thépaut JN (2020) The ERA5 global reanalysis. *Quart J R Meteorol Soc* 1–51. <https://doi.org/10.1002/qj.3803>

Holtslag AAM, De Bruijn EIF, Pan HL (1990) A high resolution air mass transformation model for short-range weather forecasting. *Mon Weather Rev* 118(8):1561–1575. [https://doi.org/10.1175/1520-0493\(1990\)118<1561:AHRAMT>2.0.CO;2](https://doi.org/10.1175/1520-0493(1990)118<1561:AHRAMT>2.0.CO;2)

Iturbide M, Gutiérrez J, Alves L, Bedia J, Cerezo-Mota R, Luca AD, Faria S, Gorodetskaya I, Hauser M, Herrera S, Hennessy K, Jones R, Kravovska S, Manzanas R, Martínez-Castro D, Narisma G, Pinto I, Seneviratne S, van den Hurk B, Vera C (2020) An update of IPCC physical climate reference regions for subcontinental analysis of climate model data: Definition and aggregated datasets. submitted to Earth System Science Data (ESSD)

Jacob D, Podzun R (1997) Sensitivity studies with the regional climate model REMO. *Meteorol Atmos Phys* 63(1–2):119–129. <https://doi.org/10.1007/BF01025368>

Jacob D, Elizalde A, Haensler A, Hagemann S, Kumar P, Podzun R, Rechid D, Remedio AR, Saeed F, Sieck K, Teichmann C, Wilhelm C (2012) Assessing the transferability of the regional climate model REMO to Different COordinated Regional Climate Downscaling EXperiment (CORDEX) Regions. *Atmosphere* 3(4):181–199. <https://doi.org/10.3390/atmos3010181>

Jacob D, Petersen J, Eggert B, Alias A, Christensen OB, Bouwer LM, Braun A, Colette A, Déqué M, Georgievski G, Georgopoulou E, Gobiet A, Menut L, Nikulin G, Haensler A, Hempelmann N, Jones C, Keuler K, Kovats S, Kröner N, Kotlarski S, Kriegsmann A, Martin E, van Meijgaard E, Moseley C, Pfeifer S, Preuschmann S, Radermacher C, Radtke K, Rechid D, Rounsevell M, Samuelsson P, Somot S, Soussana JF, Teichmann C, Valentini R, Vautard R, Weber B, Yiou P (2014) EURO-CORDEX: New high-resolution climate change projections for European impact research. *Reg Environ Change* 14(2):563–578. <https://doi.org/10.1007/s10113-013-0499-2>

Jones CD, Hughes JK, Bellouin N, Hardiman SC, Jones GS, Knight J, Liddicoat S, O'Connor FM, Andres RJ, Bell C, Boo KO, Bozzo A, Butchart N, Cadule P, Corbin KD, Doutriaux-Boucher M, Friedlingstein P, Gornall J, Gray L, Halloran PR, Hurtt G, Ingram WJ, Lamarque JF, Law RM, Meinshausen M, Osprey S, Palin EJ, Parsons Chini L, Raddatz T, Sanderson MG, Sellar AA, Schurer A, Valdes P, Wood N, Woodward S, Yoshioka M, Zerroukat M (2011) The hadgem2-es implementation of cmip5 centennial simulations. *Geosci Model Dev* 4(3):543–570. <https://doi.org/10.5194/gmd-4-543-2011>

Karmalkar AV (2018) Interpreting results from the NARCCAP and NA-CORDEX ensembles in the context of uncertainty in regional climate change projections. *Bull Am Meteorol Soc* 99(10):2093–2106. <https://doi.org/10.1175/BAMS-D-17-0127.1>

Kjellström E, Nikulin G, Strandberg G, Christensen OB, Jacob D, Keuler K, Lenderink G, van Meijgaard E, Schär C, Somot S, Sørland SL, Teichmann C, Vautard R (2018) European climate change at global mean temperature increases of 1.5 and 2° C above pre-industrial conditions as simulated by the EURO-CORDEX regional climate models. *Earth Syst Dyn* 9(2):459–478. <https://doi.org/10.5194/esd-9-459-2018>

Knist S, Goergen K, Buonomo E, Christensen OB, Colette A, Cardoso RM, Fealy R, Fernández J, García-Díez M, Jacob D, Kartsios S, Katragkou E, Keuler K, Mayer S, van Meijgaard E, Nikulin G, Soares PMM, Sobolowski S, Szepszo G, Teichmann C, Vautard R, Warrach-Sagi K, Wulfmeyer V, Simmer C (2017) Land-atmosphere coupling in EURO-CORDEX evaluation experiments. *J Geophys Res Atmos* 122(1):2016JD025,476. <https://doi.org/10.1002/2016JD025476>

Kulkarni A, Sabin TP, Chowdary JS, Rao KK, Priya P, Gandhi N, Bhaskar P, Buri VK, Sabade SS, Pai DS, Ashok K, Mitra AK, Niyogi D, Rajeevan M (2020) Precipitation Changes in India. Springer Singapore, Singapore, pp 47–72

Lohmann U, Roeckner E (1996) Design and performance of a new cloud microphysics scheme developed for the ECHAM4 general circulation model. *Clim Dyn* 12:557–572

Louis JF (1979) A parametric model of vertical eddy fluxes in the atmosphere. *Bound Layer Meteorol* 17(2):187–202

Lucas-Picher P, Laprise R, Winger K (2017) Evidence of added value in North American regional climate model hindcast simulations using ever-increasing horizontal resolutions. *Clim Dyn* 48(7):2611–2633. <https://doi.org/10.1007/s00382-016-3227-z>

Mann HB, Whitney DR (1947) On a test of whether one of two random variables is stochastically larger than the other. *Ann Math Statist* 18(1):50–60. <https://doi.org/10.1214/aoms/1177730491>

Max Planck Institute for Meteorology (2006) Climate Data Operators. <http://code.zmaw.de/projects/cdo> Accessed on 6 Oct 2018. <http://code.zmaw.de/projects/cdo>

McSweeney CF, Jones RG, Lee RW, Rowell DP (2015) Selecting CMIP5 GCMs for downscaling over multiple regions. *Clim Dyn* 44(11–12):3237–3260. <https://doi.org/10.1007/s00382-014-2418-8>

Nordeng TE (1994) Extended versions of the convective parametrization scheme at ECMWF and their impact on the mean and transient activity of the model in the tropics. Tech. rep., ECMWF Research Department, European Centre for Medium Range Weather Forecasts, Reading, UK

Pal JS, Small EE, Eltahir EAB (2000) Simulation of regional-scale water and energy budgets: representation of subgrid cloud and precipitation processes within regcm. *J Geophys Res Atmos* 105(D24):29,579–29,594. <https://doi.org/10.1029/2000JD900415>

Pfeifer S (2006) Modeling cold cloud processes with the regional climate model REMO. PhD thesis, University of Hamburg

Prein AF, Gobiet A, Truhetz H, Keuler K, Goergen K, Teichmann C, Fox Maule C, van Meijgaard E, Déqué M, Nikulin G, Vautard R, Colette A, Kjellström E, Jacob D (2016) Precipitation in the EURO-CORDEX 0.11° C and 0.44° C simulations: high resolution, high benefits? *Clim Dyn* 46(1–2):383–412. <https://doi.org/10.1007/s00382-015-2589-y>

Remedio AR, Teichmann C, Buntemeyer L, Sieck K, Weber T, Rechid D, Hoffmann P, Nam C, Kotova L, Jacob D (2019) Evaluation of new CORDEX simulations using an updated Köppen-Trewartha climate classification. *Atmosphere* 10(11):726. <https://doi.org/10.3390/atmos10110726>

Ruane AC, Teichmann C, Arnell NW, Carter TR, Ebi KL, Frieler K, Goodess CM, Hewitson B, Horton R, Kovats RS, Lotze HK, Mearns LO, Navarra A, Ojima DS, Riahi K, Rosenzweig C, Themessl M, Vincent K (2016) The vulnerability, impacts, adaptation and climate services advisory board (viacs ab v1.0) contribution to cmip6. *Geosci Model Dev* 9(9):3493–3515. <https://doi.org/10.5194/gmd-9-3493-2016>

Solman SA, Blázquez J (2019) Multiscale precipitation variability over South America: analysis of the added value of CORDEX RCM simulations. *Clim Dyn* 53(3):1547–1565. <https://doi.org/10.1007/s00382-019-04689-1>

Tangang F, Chung JX, Juneng L, Supari S, Salimun E, Ngai ST, Jamaluddin AF, Mohd MSF, Cruz F, Narisma G, Santisirisomboon J, Ngo-Duc T, Tan PV, Singhru P, Gunawan D, Aldrian E, Sopaheluwakan A, Grigory N, Remedio ARC, Sein DV, Hein-Griggs D, McGregor JL, Yang H, Sasaki H, Kumar P (2020) Projected future changes in rainfall in southeast asia based on cordex-sea multi-model simulations. *Clim Dyn*. <https://doi.org/10.1007/s00382-020-05322-2>

Taylor KE, Stouffer RJ, Meehl GA (2012) An overview of cmip5 and the experiment design. *Bull Am Meteorol Soc* 93(4):485–498. <https://doi.org/10.1175/BAMS-D-11-00094.1>

Tebaldi C, Arblaster JM, Knutti R (2011) Mapping model agreement on future climate projections. *Geophys Res Lett* 38(23):1–5. <https://doi.org/10.1029/2011GL049863>

Teichmann C, Eggert B, Elizalde A, Haensler A, Jacob D, Kumar P, Moseley C, Pfeifer S, Rechid D, Remedio A, Ries H, Petersen J, Preuschmann S, Raub T, Saeed F, Sieck K, Weber T (2013) How does a regional climate model modify the projected climate change signal of the driving GCM: a study over different CORDEX regions using REMO. *Atmosphere* 4(2):214–236. <https://doi.org/10.3390/atmos4020214>

Teichmann C, Bülow K, Otto J, Pfeifer S, Rechid D, Sieck K, Jacob D (2018) Avoiding extremes: Benefits of staying below $+1.5^{\circ}\text{C}$ compared to $+2.0^{\circ}\text{C}$ and $+3.0^{\circ}\text{C}$ global warming. *Atmosphere* 9(4). <https://doi.org/10.3390/atmos9040115>

Tiedtke M (1989) A comprehensive mass flux scheme for cumulus parameterization in large-scale models. *Mon Weather Rev* 117(8):1779–1800. 10.1175/1520-0493(1989)117<1779:ACMFSF>2.0.CO;2

Vautard R, Gobiet A, Sobolowski S, Kjellström E, Stegehuis A, Watkiss P, Mendlík T, Landgren O, Nikulin G, Teichmann C, Jacob D (2014) The european climate under a 2°C global warming. *Environ Res Lett* 9(3):034,006. <https://doi.org/10.1088/1748-9326/9/3/034006>

Watanabe M, Suzuki T, Oishi R, Komuro Y, Watanabe S, Emori S, Takemura T, Chikira M, Ogura T, Sekiguchi M, Takata K, Yamazaki D, Yokohata T, Nozawa T, Hasumi H, Tatebe H, Kimoto M (2010) Improved climate simulation by MIROC5: mean states, variability, and climate sensitivity. *J Clim* 23(23):6312–6335. <https://doi.org/10.1175/2010JCLI3679.1>

Weber T, Bowyer P, Rechid D, Pfeifer S, Raffaele F, Remedio AR, Teichmann C, Jacob D (2020) Analysis of compound climate extremes and exposed population in africa under two different emission scenarios. *Earth's Future* 8(9):e2019EF001,473. <https://doi.org/10.1029/2019EF001473>

Publisher's Note Springer Nature remains neutral with regard to jurisdictional claims in published maps and institutional affiliations.